Decoding cytokine networks in ulcerative colitis to identify pathogenic mechanisms and therapeutic targets

Marton Olbei[1], Isabelle Hautefort[1,2,3,4], John P. Thomas[1,5], Luca Csabai[6], Balazs Bohar[1], Sandra S. Koigi[4], Hajir Ibraheim[1], Aamir Saifuddin[1], Diana Coman[7], Emma Højmose Kromann[7], Joana F. Neves[7], Diana Papp[4], Nick Powell[1], Dezso Modos[1,3], Tamas Korcsmaros[1,2,3,4*]

[1]Department of Metabolism, Digestion and Reproduction, Imperial College London; London, W12 0NN, United Kingdom. [2]Earlham Institute; Norwich, NR4 7UZ, United Kingdom. [3]Quadram Institute; Norwich, NR 47UZ, United Kingdom. [4]NIHR Imperial BRC Organoid Facility, Imperial College London; London, W12 0NN, United Kingdom. [5]UKRI MRC Laboratory of Medical Sciences, Hammersmith Hospital Campus; London, W12 0NN, UK. [6]Department of Genetics, Eotvos Lorand University; Budapest, 1117, Hungary. [7]Centre for Host Microbiome Interactions, King's College London, London, WC2R 2LS, United Kingdom.

[*]Corresponding author. Email: t.korcsmaros@imperial.ac.uk

Abstract

Ulcerative colitis (UC) is a chronic inflammatory disorder of the gastrointestinal tract that is characterized by dysregulated cytokine signaling. Despite the advent of advanced therapies targeting cytokine signaling, treatment outcomes for UC patients remain suboptimal. Hence, there is a pressing need to better understand the complexity of cytokine regulation in UC by comprehensively mapping the interconnected cytokine signaling networks that are perturbed in UC patients. To address this, we undertook systems immunology modelling of single-cell transcriptomics data from colonic biopsies of treatment-naive and treatment-exposed UC patients to build complex cytokine signaling networks underpinned by putative cytokine-cytokine interactions. The generated cytokine networks effectively captured known physiologically relevant cytokine-cytokine interactions, which we validated in vitro in UC patient–derived colonic epithelial organoids and with organoids co-cultured with innate lymphoid cells. These networks revealed previously unappreciated aspects of UC pathogenesis, including a cytokine subnetwork that is unique to treatment-naive UC patients, the identification of cytokines with altered

interaction patterns across UC disease states (including IL-22, TL1A, IL-23A, and OSM), cytokine-cytokine interactions that were mediated by specific members of the Janus-associated kinase (JAK) family, and the positioning of TL1A as an important upstream regulator of TNF and IL-23A (the two cytokines currently targeted by approved UC drugs) and as a potential therapeutic target. Together, these findings open several avenues for guiding future cytokine-targeting therapeutic approaches in UC, and the presented methodology can be readily applied to gain similar insights into other immune-mediated inflammatory diseases.

INTRODUCTION

Cytokines are key signaling molecules of the immune system that play critical roles in the regulation of the immune response. Cytokines are released by various cell types and bind to their cognate receptors on the surface of their target cells (1). The binding of a cytokine ligand to its receptor initializes a signaling cascade, culminating in the regulation of downstream target genes, including those encoding other cytokines (2). Thus, cytokines can form complex networks of interactions, in which different cytokines regulate the production and activity of other cytokines, thereby organizing immune responses. Many of these individual cytokine-cytokine interactions are well-established in classical immune responses, such as activation of interferon-γ (IFNG) by the cytokine interleukin-12 (IL-12) as part of the T helper 1 (T_H1) cell–mediated adaptive immune response (3, 4), which in turn activates chemokines such, as CXCL10, through innate immune cells, such as monocytes (5). Such cytokine-cytokine interactions are important for maintaining the proper balance and specificity of immune responses. However, when they are dysregulated, chronic immune-mediated inflammatory disorders, such as ulcerative colitis (UC) can develop (6). UC is a major subtype of inflammatory bowel disease (IBD), which is characterized by chronic

colonic inflammation limited to the mucosal layer of the gut wall. UC causes substantial morbidity to patients, with symptoms such as bloody diarrhea, abdominal pain, and fatigue, and its prevalence is rising globally (7). UC pathogenesis is underpinned by an imbalance of pro- and anti-inflammatory cytokine production, leading to dysregulated cytokine signaling, chronic inflammation, and ultimately tissue damage (8–10).

Many of the currently available biologic therapies for UC aim to target key dysregulated cytokines. These include anti–tumor necrosis factor (TNF) agents, such as infliximab and adalimumab, biologics targeting the common p40 subunit of IL-12 and IL-23, such as ustekinumab, as well as drugs targeting the p19 subunit of IL-23, such as mirikizumab. In addition, small-molecule drugs inhibiting Janus-associated kinase (JAK) signaling (such as filgotinib, tofacitinib, and upadacitinib) have been established in clinical practice, which underpin multiple cytokines and immune signaling cascades (11). The addition of these advanced therapies in the therapeutic armamentarium has substantially increased the prospects for UC patients, resulting in better outcomes and quality of life (12). However, despite this, a substantial therapeutic ceiling exists, in which 50 to 70% of the patient population fails to respond or becomes resistant to these treatments (13–15). This has led experts to call for new therapeutic strategies targeting multiple cytokines of interest, such as combination biologic therapies. Indeed, clinical trials such as the VEGA trial, which is evaluating the combination therapy of anti-TNF and anti–IL-23, are currently underway to test this hypothesis (16). As such, there is an increased need to understand the complexity of cytokine regulation in IBD, to disentangle how treatment affects cytokine signaling, and how this information can be leveraged to offer alternative perturbation points (17, 18). However, systems-

level analyses collecting and modelling the totality of these cytokine-cytokine interactions have been few and far between (19, 20).

We previously established CytokineLink, a systems biology framework that maps cytokine-cytokine interactions based on ligand and receptor expression (19). Although CytokineLink enables the exploration of these interactions, it lacks integration of the intracellular signaling cascades stimulated by cytokine-receptor binding. Here, we advanced our network models by incorporating intracellular signaling data derived from single-cell gene expression profiles of UC patients (21), enhancing the accuracy and depth of the cytokine-cytokine interaction analysis. Using a newly developed integrated pipeline, we reconstructed condition- and treatment-specific cytokine networks of the colonic mucosa in UC patients and non-IBD controls. Comparative analysis of these cytokine networks captured important cytokine regulation differences between treatment-naive UC patients, treatment-exposed UC patients, and non-IBD controls. The analysis identified the cytokines with the most altered interactions in UC, a unique cytokine subnetwork in treatment-naive patients, and provided insights into cytokine signaling hierarchies. Our study also highlighted the pervasive role of Janus-associated kinase (JAK) signaling in cytokine interactions and the specificity of JAK paralogs in UC. Together, this systems immunology approach provides particular insights into UC pathogenesis with substantial translational potential and can be used to delineate cytokine signaling in other immune-mediated inflammatory diseases (IMIDs).

RESULTS

Mapping the cytokine interaction networks driving UC

To better understand how cytokines may regulate each other in UC, we generated cytokine-cytokine interaction networks from single-cell RNA sequencing (scRNA-seq) data derived from colonic biopsies of UC patients and non-IBD controls. To achieve this, we used data from the single-cell RNA-Seq compendium for IBD, scIBD (21), which provided us curated, batch-corrected, and integrated scRNA-seq data from multiple studies, improving the power of our analysis. In total, we used data from 85 UC patients and 43 non-IBD controls from scIBD. The scRNA-seq data from the UC patients were stratified based on the inflammation status of the colonic biopsies and further grouped based on whether the patients had undergone treatment (with immunomodulators, advanced therapies, or both) or were treatment-naive using the available supplementary materials of the original studies.

We harnessed the computational methods of NicheNet to infer ligand–target gene interactions from the scRNA-seq data (22). This approach incorporates a prior model regarding intracellular signaling and gene regulatory networks to predict whether the binding of ligands to target receptors can modulate the expression of target genes. This was important to capture the potential intracellular mechanisms connecting upstream and downstream cytokines and map the chain of events consisting of cytokine → receptor → signaling proteins → transcription factors → cytokine-encoding genes (Fig. 1A). Because we focused on cytokine-cytokine interactions, we restricted both the upstream ligands and the downstream target genes to known cytokine genes as defined in established systems immunology databases. This enabled us to construct networks of cytokine-cytokine interactions from the scRNA-seq data.

The datasets within the scIBD atlas differentiate the UC subtypes based on inflammation status, containing samples from both inflamed and noninflamed locations of the gastrointestinal tract. To add further dimensionality to the generated networks, we delineated a cluster of treatment-naive inflamed UC samples from the publicly available supplementary materials of the included datasets. Hierarchical clustering of the generated cytokine networks revealed that the networks clustered according to disease status (UC vs. non-IBD control), treatment exposure, and inflammation status (Fig. 1B). For each condition, the generated networks were comparable in size and shared 43% of their interactions across all states. We assessed the local and global importance of nodes using degree (that is, local importance, number of neighbors) and betweenness centrality (that is, global importance), respectively. Including interactions from all of the cytokine networks, the highest degree cytokines (cytokines with the largest number of interactions) were IL1B, CCL2, TNF, IFN-γ and IL6 (Fig. 1C). The same five cytokines also achieved the highest betweenness centrality measures (albeit in a slightly different order: IL1B, CCL2, IFNG, TNF, and IL6), highlighting not only their local, but also their global importance in cytokine communication.

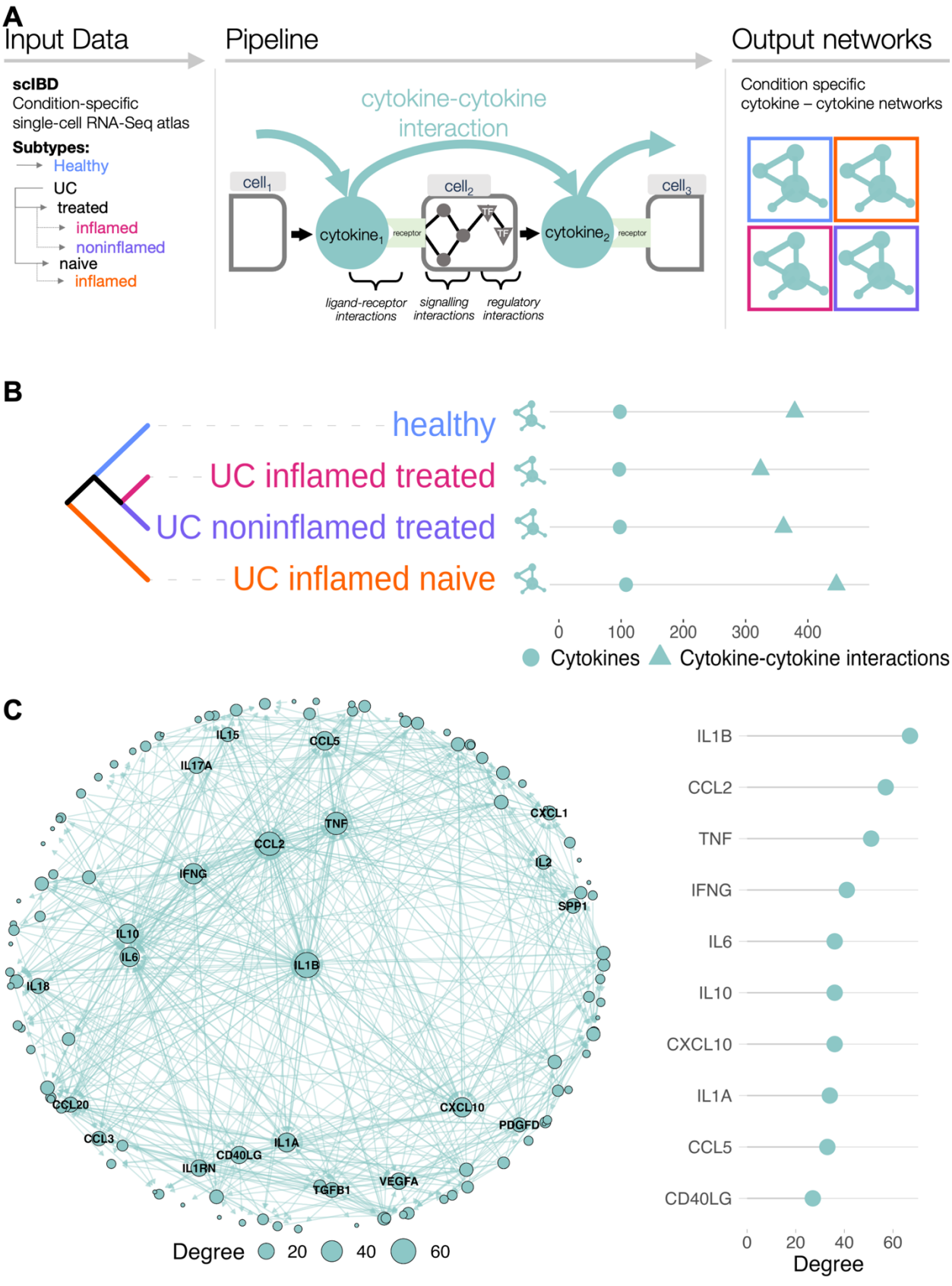
A
Input Data
Pipeline
Output networks
scIBD
Condition-specific
single-cell RNA-Seq atlas
Subtypes:
Healthy
UC
treated
inflamed
noninflamed
naive
inflamed
cytokine-cytokine
interaction
cell1
cell2
cell3
cytokine1
receptor
TF
TF
cytokine2
receptor
ligand-receptor
interactions
signalling
interactions
regulatory
interactions
Condition specific
cytokine – cytokine networks
B
healthy
UC inflamed treated
UC noninflamed treated
UC inflamed naive
0
100
200
300
400
Cytokines
Cytokine-cytokine interactions
C
IL15
CCL5
IL17A
CXCL1
TNF
CCL2
IL2
IFNG
SPP1
IL10
IL6
IL1B
IL18
CCL20
CXCL10
PDGFD
CCL3
IL1A
CD40LG
IL1RN
TGFB1
VEGFA
Degree
20
40
60
IL1B
CCL2
TNF
IFNG
IL6
IL10
CXCL10
IL1A
CCL5
CD40LG
0
20
40
60
Degree

Figure 1. Generating condition-specific cytokine networks in ulcerative colitis. A: The computational pipeline processes data from the single-cell RNA-Seq inflammatory bowel disease atlas scIBD. Based on available metadata, we delineated a novel cluster of inflamed UC samples ("inflamed-naive" in the above figure) from patients who did not receive any immunomodulatory or advanced therapies. Data was processed using NicheNet, with the gene set of interest set to a list of cytokines. It connected active cytokine ligands to their putative cytokine targets, resulting in condition-specific cytokine networks. **B**: Hierarchical clustering of networks according to disease and treatment status. The generated networks are comparable in size, with the inflamed treatment naive network having the largest number of interactions. **C**: Analysing all generated interactions reveals the highest degree cytokines in the cytokine networks. The centrality network layout emphasises betweenness centrality, with the most central cytokines positioned closer to the centre.

Cytokine networks capture physiologically relevant cytokine-cytokine interactions

To confirm the physiological relevance of the cytokine networks, we tested our results with a large independent compendium focusing on immune cells and with an organoid experiment focusing on UC patient–derived epithelial cells, as well as a co-culture model containing group 1 innate lymphoid (ILC1) cells and organoids to capture immune-epithelial crosstalk on a protein level. First, we compared our data to the published Immune Dictionary resource (23). Briefly, the Immune Dictionary encompasses the responses of 17 murine immune cell types to 86 cytokines one-by-one. We tested the target overlap and set the similarity of each matching source (that is, upstream) cytokine from our cytokine-cytokine interaction networks (Fig. 2A). Forty-five cytokines caused differential expression of other cytokines in the Immune Dictionary resource. Of those 45, 20 cytokines were also source nodes in our networks, targeting other cytokines. Comparing the sets of targeted cytokines in the Immune Dictionary with the UC cytokine network model, 12 of 20 individual cytokines (60%) had a significant overlap in their targets between the Immune Dictionary results and our computational model (hypergeometric test, FDR <= 0.05). Of the remaining 25 comparable cytokines with the Immune Dictionary resource, 17 were present as nodes in our cytokine networks as targets of other cytokines (but not as source molecules targeting

other cytokines). Eight cytokines were not among our search parameters. The substantial overlap between key targets in our constructed cytokine-cytokine interaction networks and those in the Immune Dictionary resource suggest that our networks are likely to be physiologically relevant. We prepared a network representation of the experimentally validated and predicted interactions in the UC inflamed naïve network (fig. S1). However, we acknowledge that not all interactions could not be captured because of inherent differences in the sets of cytokines between both studies. For example, the current study involves many chemokines and growth factors that were not included in the Immune Dictionary resource. Furthermore, the cellular compartments of the producing cells also differed, as the Immune Dictionary primarily focused on immune cell types from lymph nodes, whereas the UC cytokine networks presented here were generated from colonic tissue samples from patients involving the immune, epithelial, and stromal compartments. Finally, the Immune Dictionary was generated from murine tissues, and important differences exist between the mouse and human immune systems (24–26).

To further validate our results, we generated inflamed and non-inflamed colonic epithelial organoids from UC patients to model inflammation and recapitulate the inflamed and non-inflamed interactions in vitro. Organoids were treated with a mixture of pro-inflammatory mediators (IL-1B, TNF, and Flagellin) that reproduce a similar transcriptomic phenotype to that of the inflamed epithelium in IBD patients to generate inflamed organoids (27). We then treated both inflamed and non-inflamed organoids with IFN-γ. This proinflammatory cytokine plays a crucial role in intestinal inflammation, is released by adaptive immune cells, and acts on the intestinal epithelial layer (28). The effects of IFN-γ on these organoids were captured by RNA-seq. We generated a simplified UC cytokine network, comprising interactions exclusively between

epithelial cell types found in organoids, and classified the cytokine targets of IFN-γreleased by these cells as a custom IFN-γgene set. Gene set enrichment analysis (GSEA) of the IFN-γtarget cytokine gene set identified a statistically significant enrichment of the IFN-γtargets in the differential gene expression results (Fig. 2B). To validate the healthy cytokine networks, in addition to the UC cytokine networks, we compared the predictions with data from studies by Pavlidis et al (*29*, *30*), where we previously treated healthy colonic organoids with different cytokines and captured their responses by bulk RNA-seq. We found a significant enrichment of the predicted cytokine targets between the differentially expressed genes after the treatment of healthy organoids with IFN-γ, TNF, and IL-17, respectively. The GSEA results showing the enrichment of cytokine targets in both the UC patient derived and healthy organoids are shown on Figure 2C.

We also quantified the degree to which our approach captured cytokine interactions involved in the crosstalk between epithelial and immune cell types and predicted the effects of endogenous cytokine production in addition to direct external cytokine stimulation at a protein level. To this end, we measured changes in cytokine protein concentrations in supernatants from healthy small intestinal organoids that were co-cultured with or without ILC1 cells. Based on previous studies, we expected the ILC1 cells to produce three key cytokines: TGF-β1 (31), IFN-γ, and TNF (32). Thus, we tested whether our model could predict changes in the concentrations of the downstream cytokine targets of TGF-β1, IFN-γ, and TNF produced by epithelial cells of the organoids after being co-cultured with ILC1 cells. Of the 14 tested downstream cytokines, eight (57%) showed significant changes in concentration after co-culturing (Fig. 2D, fig. S3).

Finally, to ascertain whether the predictions were the product of the scRNA-seq data used rather than the prior knowledge resource that was used, we generated matching state-specific cytokine networks after randomizing gene labels in the integrated scRNA-seq data (scIBD), and compared the distributions of degree and betweenness centrality values between the original and shuffled networks (table S2). All Wilcoxon Rank Sum tests indicated statistically significant differences, with the only exception being the betweenness centrality distributions of the “healthy” networks, where the $P = 0.09$.

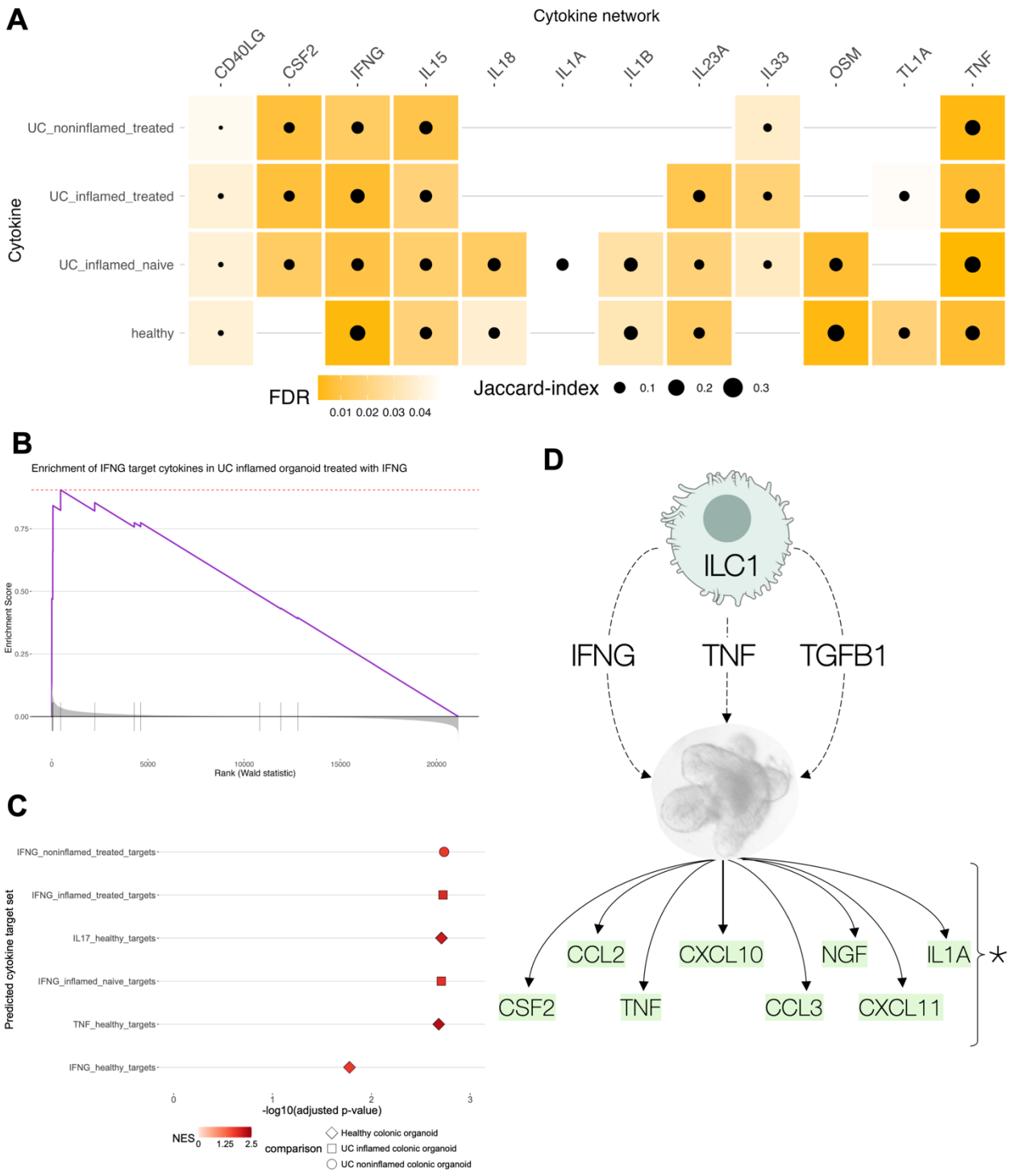

Figure 2. Validation of cytokine–cytokine interactions. A: Comparison of target sets between predicted interactions and differential expression results from the Immune Dictionary resource (Cui et al) 12/20 shared source cytokines have significantly overlapping target sets. **B**: Enrichment plot showing the enrichment of IFNG targets in differentially expressed genes from patient-derived inflamed colonic organoids (n = 4) treated with IFNG. **C**: Enrichment of target

sets of multiple cytokines in inflamed, noninflamed and healthy colonic organoid transcriptomics data. **D**: Downstream cytokines with significantly changing protein concentration levels following co-culturing with ILC1 cells (n=3 for standalone, n = 4 for ILC1 co-cultures). We observed a significant change in protein concentration for 57% of predicted targets (Wilcoxon Rank Sum test, p-value <= 0.05). Supplementary Figure 3 details p-values for all measured cytokines.

A specific cytokine subnetwork distinguishes treatment-naive from treatment-exposed inflamed UC tissues

Leveraging the supplementary materials of the original studies from the scRNA-seq datasets in scIBD, we generated a cytokine-cytokine interaction network from inflamed biopsies of seven treatment-naive UC patients, that is, individuals who had not been exposed to immunomodulators or advanced therapies (for sample IDs and dataset details, see the Materials and Methods). Thus, the network we constructed from these patients likely reflects the nature of cytokine interactions in active UC before therapeutic intervention. We determined the Jaccard index for each interaction based on the cell types involved, indicating the similarity of compared sets, to determine whether there were differences in the putative cell types mediating these cytokine interactions. We established this in both the treatment-naive and treatment-exposed patient groups, compared to non-IBD controls. We analyzed the distribution of these scores in the inflamed treatment-naive and inflamed treatment-exposed networks in UC, with the inflamed treatment-naive interactions exhibiting a lower median Jaccard index (Fig. 3A). This indicates that the cell types contributing to these inflamed treatment-naive interactions were more different than in the inflamed treatment-exposed networks compared to the healthy state (median inflamed-naive = 0.27, median inflamed-treated = 0.38, Wilcoxon-Rank Sum test P value < 1.6×10^{-6}). There were 17 cell types shared

between inflamed-treated and healthy conditions that were not present in the inflamed-naive condition (fig. S4).

We next sought to understand the differences in cytokines mediating these interactions during active disease in the treatment-exposed and treatment-naive groups. We compared the number of neighbors (degree values) of the cytokines present in the networks between both conditions (Fig. 3B). We observed that after exposure to immunomodulators or advanced therapies, all of the cytokines lost interactions with their immediate neighbors, reducing their local importance. A comparison of their global importance, as assessed through betweenness centrality, showed a similar trend, with the exception of three cytokines (CD40LG, IFN-γ, and CCL11), which became more central after treatment. These findings suggest that exposure to immunomodulators or advanced therapies restructures cytokine networks in UC, reducing both the local and global importance of key cytokines that mediate cytokine-cytokine interactions in active disease.

To better understand the cytokine–cytokine interactions underpinning active UC without any modulation from immunomodulators or advanced therapies, we visualized the interactions that were unique to the treatment-naive group. Eighty-three interactions were unique to the UC inflamed treatment-naive network, representing 19% of the total interactions in this network. Seventy-seven of these interactions formed a connected subnetwork. We visualized these treatment naive–specific interactions with a hierarchical layout, which enabled us to determine the chain of cytokine interactions involved in the treatment-naive inflamed colonic mucosa. We assembled the hierarchical structure of these state-specific interactions, and the largest sources and sinks unique to the condition (Fig. 3C). The highest in-degree nodes of this subnetwork were the

important pro-inflammatory cytokines TNF, IL-1β, and IL-6, as well as the chemokine CCL2 (Fig. 3C bottom right). The most promiscuous source cytokine was IL-1α, which targeted 17 other cytokines, highlighting its important role in inflammation (Fig. 3C, bottom right) (33, 34). IL-1α was followed by RETN (resistin), an inflammatory marker in IBD with known roles in the inflammatory response (35, 36). Thus, our systems immunology cytokine-modelling captured prototypical cytokines associated with UC pathogenesis, while providing insights into their hierarchical relationships.

We next focused on cytokines that are currently directly targeted by biologics in UC. The most commonly used biologic agents in UC are anti-TNF agents (37). We found that TNF was one of the highest degree nodes in the treatment-naive inflamed UC cytokine network, interacting with 37 other cytokines, that is, 34% of the cytokine network members. We analyzed the UC-specific inputs from multiple proinflammatory and regulatory cytokines targeting TNF, with the incoming CCL21, IL-10, IL-1α, RETN, and TNFSF11 interactions only appearing in the UC treatment-naive condition. As for outgoing interactions of TNF, TNF targeted itself and PDGFB in the treatment-naive inflamed condition, the latter cytokine previously shown to be an important driver of fibrosis in IBD (Fig. 3E) (38). The cytokine IL-23A is another important target of biologic treatment in UC (39), either through drugs (for example, ustekinumab) targeting its p40 subunit shared with IL-12A (not active in network), or also through drugs targeting its p19 subunit (for example, mirikizumab). IL-23A had four interactions unique to the treatment-naive state: upstream inputs from IL-1α and IL-17A, and downstream targets to the IL-10 family cytokines, IL-19 and IL-24 (Fig. 3E). As with most other cytokines (Fig. 3B), the degree and betweenness centrality values for IL-23A were reduced in the treatment-exposed inflamed condition.

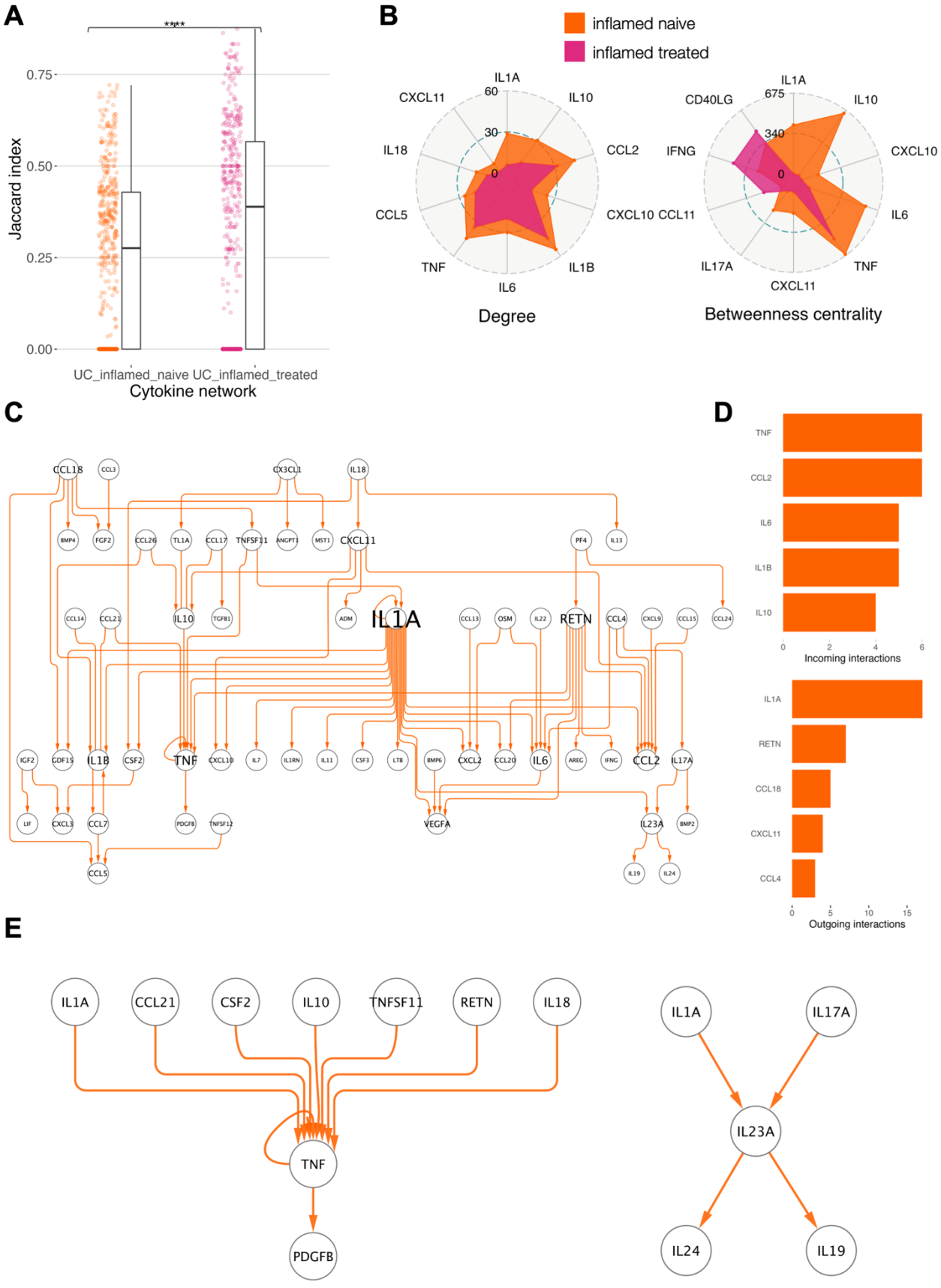
A
****
0.75
0.50
0.25
0.00
Jaccard index
UC_inflamed_naive
UC_inflamed_treated
Cytokine network
B
inflamed naive
inflamed treated
IL1A
IL10
CCL2
CXCL10
CCL11
IL6
IL1B
TNF
IL18
CCL5
CXCL11
60
30
0
Degree
CD40LG
IFNG
IL17A
675
340
Betweenness centrality
C
CCL18
CCL3
CX3CL1
IL18
BMP4
FGF2
CCL26
TL1A
CCL17
TNFSF11
ANGPT1
MST1
CXCL11
PF4
IL13
CCL14
CCL21
IL10
TGFB1
ADM
IL1A
CCL13
OSM
IL22
RETN
CCL4
CXCL9
CCL15
CCL24
IGF2
GDF15
IL1B
CSF2
TNF
CXCL10
IL7
IL1RN
IL11
CSF3
LTB
BMP6
CXCL2
CCL20
IL6
AREG
IFNG
CCL2
IL17A
LIF
CXCL3
CCL7
PDGFB
TNFSF12
VEGFA
IL23A
BMP2
CCL5
IL19
IL24
D
TNF
CCL2
IL6
IL1B
IL10
0
2
4
6
Incoming interactions
IL1A
RETN
CCL18
CXCL11
CCL4
0
5
10
15
Outgoing interactions
E
IL1A
CCL21
CSF2
IL10
TNFSF11
RETN
IL18
TNF
PDGFB
IL1A
IL17A
IL23A
IL24
IL19

Figure 3. A specific subnetwork of cytokine-cytokine interactions characterise treatment-naive inflamed UC tissues. A: Differences in the Jaccard index distribution of cytokine–cytokine interactions. The Jaccard index quantifies the set similarity of cell types contributing to the cytokine–cytokine interaction (as source or target cells) with the healthy condition. The inflamed treatment-naive network has a lower average Jaccard index than the inflamed treatment-exposed network, indicating that the contributing cell types are more different compared to healthy than in the treated networks (median inflamed-naive = 0.27, median inflamed-treated = 0.38, Wilcoxon-Rank Sum test $P < 1.6e-06$). **B**: Degree and betweenness centrality differences between inflamed treatment-naive and treatment-exposed networks. The highest degree cytokines all lose interactors in the treatment-exposed condition, and the highest betweenness centrality cytokines become less central, except CD40LG, IFNG and CCL11. **C**: An inflamed treatment-naive condition-specific subnetwork in ulcerative colitis. **D**: Cytokines with the highest number of incoming interactions in the treatment-naive subnetwork (top) and cytokines with the highest number of outgoing interactions (bottom). **E**: Cytokines with active signals currently targeted by biologic agents (TNF, IL23A) in the treatment-naive state

Network rewiring analysis pinpoints cytokines with the most varying interactomes across inflammatory states in UC

To characterize the distinct and shared properties of the generated cytokine networks, and to identify both divergent and conserved cytokine interactions across states, we initially analyzed the networks with the DyNet network rewiring algorithm (40). This approach enabled us to identify the cytokines present in all networks that had the most variable neighborhoods (Fig. 4A). The top-ranking rewired cytokines (Fig. 4B) included IL-22, TL1A (encoded by *TNFSF15*), IL-23A, and OSM, which have been implicated in the pathogenesis of IBD (11, 14, 30). We also analyzed the detailed interactomes of IL-22 and OSM (Fig. 4C). IL-22 is an IL-10–family cytokine involved in epithelial regeneration (41), and its abundance is often increased in the intestinal mucosa of IBD patients (11). IL-22 has been linked with resistance to anti–IL-12 and anti–IL-23 treatment, and it increases the abundance of proinflammatory CXC-family chemokines (30). In the inflamed naive cytokine network, IL-22 was targeted by IL-23A (42) and directly regulated CXCL6 and, through CCL2, affects CXCL1 to CXCL5 (fig. S5). It sends further direct UC-specific interactions to IL6, CCL20, and VEGFA. OSM is an IL-6–family cytokine whose abundance is often increased in IBD

patients (43). OSM is a driver of inflammatory processes, and it increases the production of IL-6 and proinflammatory chemokines (14), as captured by our model. OSM is also linked with resistance to anti-TNF treatment (14). In addition to targeting the aforementioned proinflammatory cytokines and chemokines, OSM also targeted AREG in the treatment naive cytokine network, a cytokine that promotes intestinal fibrosis in experimental colitis and in patients with Crohn's disease, a different subtype of IBD (44).

After the rewiring analysis, to explore the shared properties of the UC networks, as opposed to their differences, we collated the interactions missing from all of the UC cytokine networks compared to the healthy state (that is, interactions that were exclusive to health), and collected interactions present in all UC cytokine networks (that is, interactions exclusive to UC) (Fig. 4D). There were 18 health-specific and 25 UC-specific interactions, regardless of treatment status or whether the sample was derived from an inflamed or non-inflamed site. We analyzed the largest connected components of these shared interactions (Fig. 3D). The central node in the graph of health-specific interactions was IL-33, an important IL-1–like alarmin responsible for initiating a response to cellular damage (45). So far, there have been conflicting reports regarding the role of IL-33 in UC, as it exerts both detrimental and protective effects in mouse models of colitis (46). In contrast, the shared UC-specific interactions formed two larger subgraphs. In the first, the upstream nodes were IL-18 and CSF2, cytokines that enhance and, in some cases, decrease the amounts of proinflammatory cytokines, such as IFN-γ, TNF, and IL-1β (11, 47–50). The second connected component was driven by IGF2, primarily targeting other growth factors, many of which were previously implicated in IBD pathogenesis (51–54).

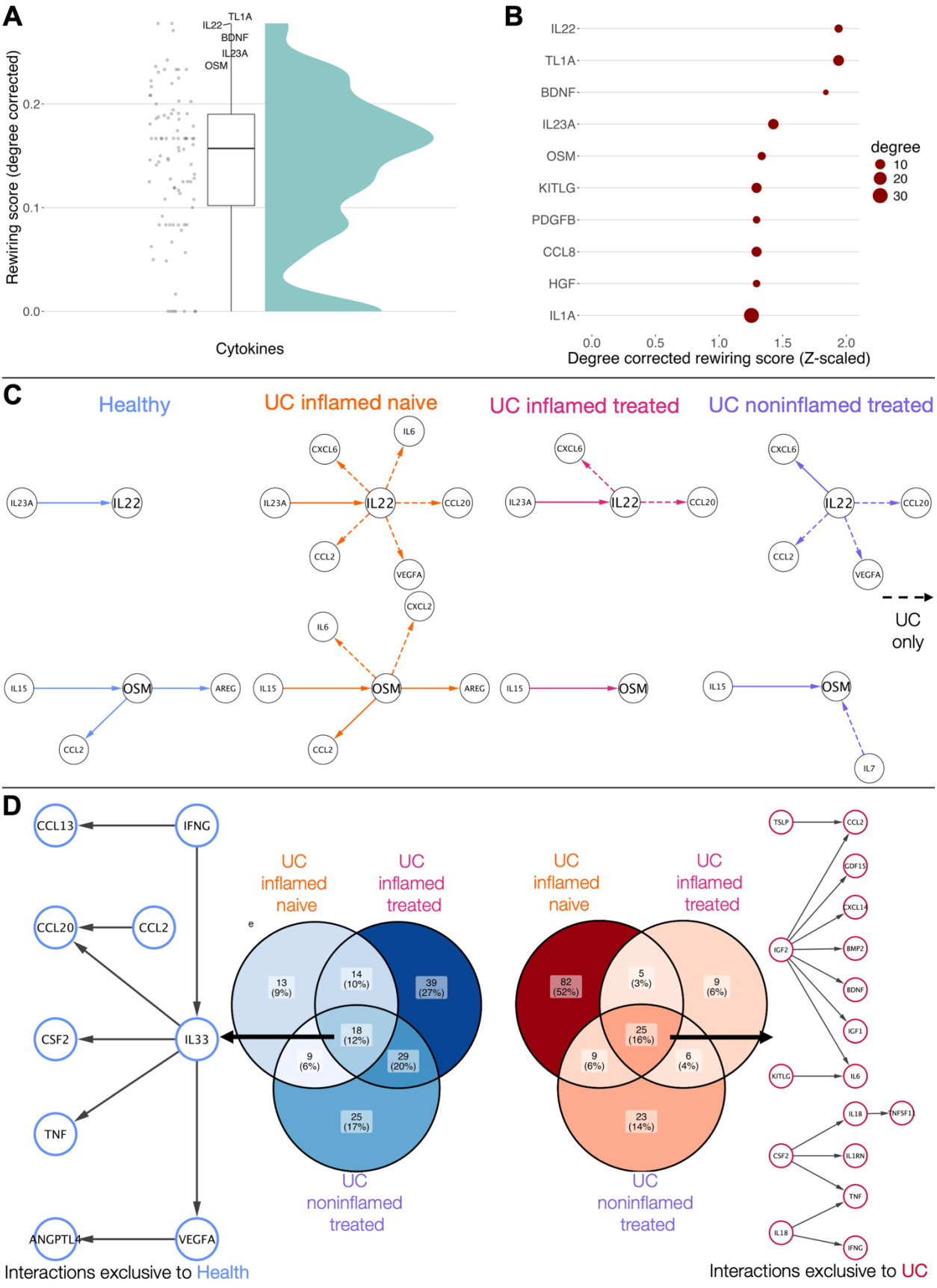
A
Rewiring score (degree corrected)
0.0
0.1
0.2
IL22
TL1A
BDNF
IL23A
OSM
Cytokines
B
IL22
TL1A
BDNF
IL23A
OSM
KITLG
PDGFB
CCL8
HGF
IL1A
degree
10
20
30
0.0
0.5
1.0
1.5
2.0
Degree corrected rewiring score (Z-scaled)
C
Healthy
UC inflamed naive
UC inflamed treated
UC noninflamed treated
IL23A
IL22
CCL20
CXCL6
IL6
CCL2
VEGFA
CXCL2
IL15
OSM
AREG
IL7
UC only
D
CCL13
IFNG
CCL20
CCL2
CSF2
IL33
TNF
ANGPTL4
VEGFA
UC inflamed naive
UC inflamed treated
UC noninflamed treated
13 (9%)
14 (10%)
39 (27%)
18 (12%)
9 (6%)
29 (20%)
25 (17%)
82 (52%)
5 (3%)
9 (6%)
25 (16%)
9 (6%)
6 (4%)
23 (14%)
Interactions exclusive to Health
TSLP
CCL2
GDF15
CXCL14
IGF2
BMP2
BDNF
IGF1
KITLG
IL6
IL1B
TNFSF11
CSF2
IL1RN
TNF
IL18
IFNG
Interactions exclusive to UC

Figure 4. Cytokine network rewiring and shared interactions. A: Distribution of degree-corrected rewiring scores. The top-scoring cytokines are highlighted. **B**: The top rewired nodes shared across all networks **C**: In-depth look at the first neighbours of rewired nodes IL22 and OSM. **D**: Missing (left) and shared (right) subnetworks in UC. The largest connected components of the missing (exclusive to healthy) and shared (exclusive to UC) interactions are shown next to the Venn-diagrams.

The JAK profiles of cytokine–cytokine interactions in UC

We next evaluated the intracellular pathways mediating cytokine-cytokine interactions in UC, specifically focusing on the JAK signaling cascade. which serves as the primary signal transduction pathway for multiple cytokines (55). JAK signaling has emerged as a crucial therapeutic target in IBD after phase III clinical trials demonstrated the efficacy of non-selective and selective JAK inhibitors for induction and maintenance therapy in UC (56). To deconvolute the specificity of JAK paralogs in cytokine signaling in UC, we captured the likely intracellular pathways connecting source cytokines to their putative target cytokine genes and collated the JAK proteins underpinning each interaction. In the UC inflamed treatment-naive network, 55% of interactions involved signaling by one or more JAKs (Fig. 5A). To assess the reliability of the captured cytokine-JAK relationships, we compared the number of correct and incorrect JAK paralog assignments for nine active cytokine ligands in the networks whose JAK preferences were reviewed previously (11). In all nine cases, the correct JAK paralogs were assigned to the signaling cytokine. However, the pipeline did not assign JAKs to intracellular pathways for a few interactions between certain cytokines (mean = 86%) (Fig. 5B). To quantify the effect of JAK paralog–specific inhibition in UC, we calculated the DyNet rewiring score of the UC inflamed treatment-naive cytokine network before and after removing cytokine-cytokine interactions that signal through each affected JAK paralog (Fig. 5C). Based on the UC inflamed treatment-naive

cytokine network, the neighborhoods of CD-40LG, IL-10, and IFN-γ were the most perturbed by the removal of JAK1-mediated interactions, indicating that JAK1-selective inhibitors, such as upadacitinib, might inhibit cytokine-cytokine interactions connecting to these cytokines. The removal of JAK1-affected edges also excluded certain nodes from the cytokine network, such as OSM and IL-22, which are associated with resistance to anti-TNF (14) and anti–IL-12/23 (30) therapies, respectively (Fig. 5D). Thus, JAK1 signaling is likely to encompass these resistance proteins, which may explain why JAK1 inhibition with upadacitinib or non-selective JAK inhibition with tofacitinib demonstrated generally consistent efficacy in both biologic naive and biologic exposed UC patients in phase III clinical trials (57, 58).

A

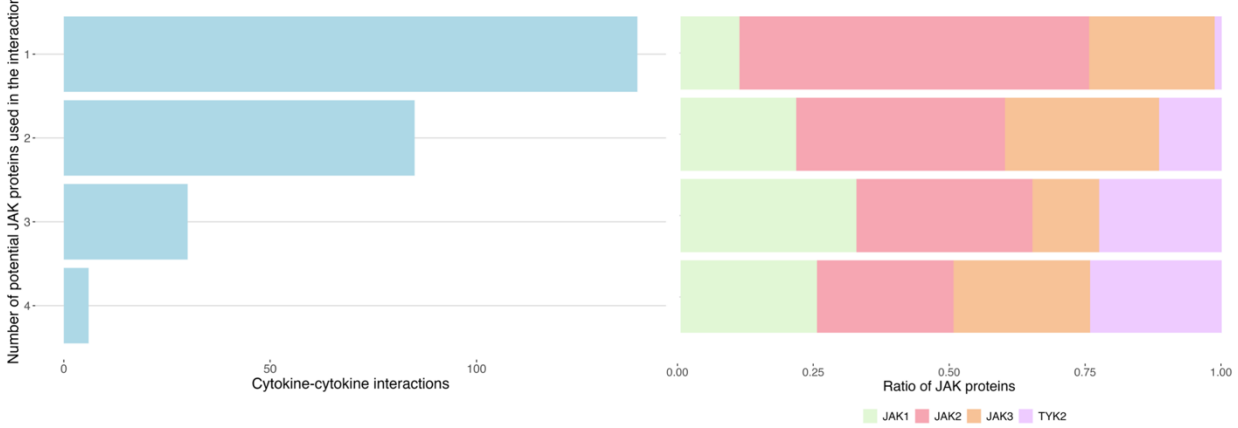

B

Cytokine	JAK1	JAK2	JAK3	TYK2	Number of interactions	Number of interactions using JAKs	Number of interactions using correct JAKs	Percentage of interactions using correct JAK	Percentage of JAK interactions using correct JAK
IL7	1	0	1	0	3	3	3	100%	100%
TSLP	1	0	1	0	3	3	3	100%	100%
OSM	1	1	0	1	4	4	4	100%	100%
IFNG	1	1	0	0	15	15	15	100%	100%
CSF2	0	1	0	0	4	4	4	100%	100%
IL23A	0	1	0	1	7	7	7	100%	100%
IL15	1	0	1	0	13	10	10	76.9%	100%
IL10	1	1	0	1	14	10	10	71.4%	100%
IL6	1	1	0	1	6	2	2	33.3%	100%

C

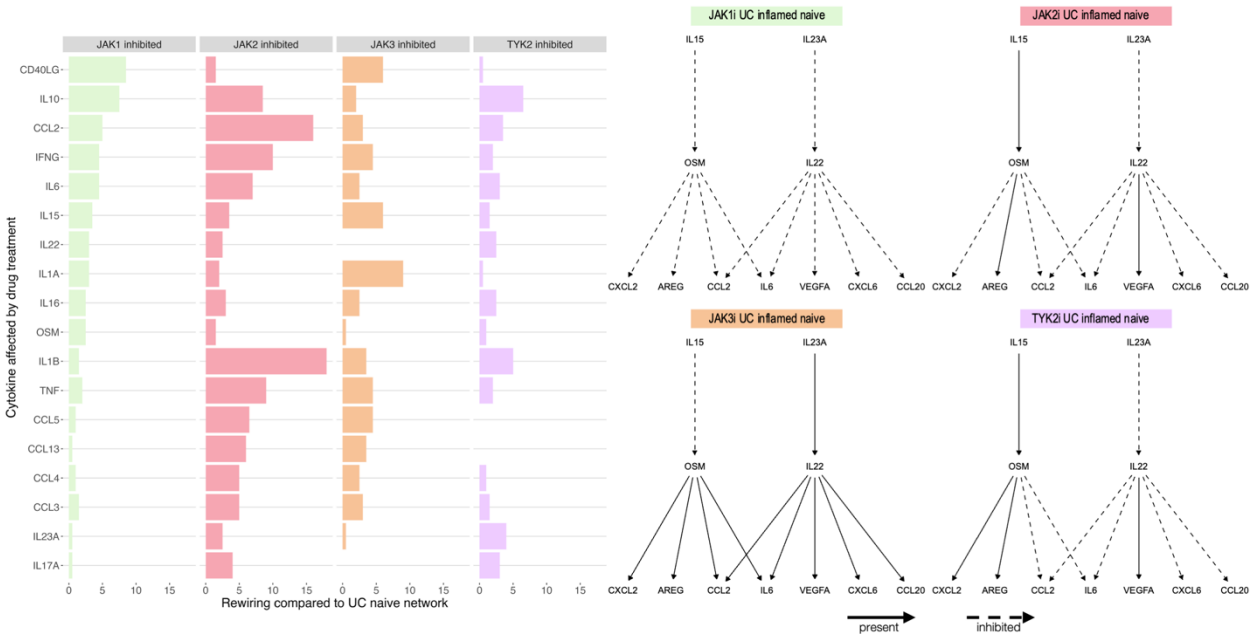

Figure 5. JAK paralogue specificity of cytokine networks. A: Number of JAK proteins used by the generated cytokine–cytokine interactions (left) and their ratio of used JAK proteins. **B**: Select cytokines with known JAK preferences, and the percentage of correctly identified JAKs in the predicted intracellular signalling pathways. **C**: DyNet rewiring compared to the inflamed-naive network following the removal of cytokine interactions mediated by JAK paralogues. Only top values are shown. **D**: Removal of JAK1 interactions excludes IL22 and OSM from the UC inflamed treatment naive cytokine network.

Drug-targeting analysis reveals TL1A as a critical cytokine target in UC

TNF, IL-23A, and IL-12A are the three cytokines currently targeted by biologics to treat UC. To better understand how and why particular cytokines might be better targets than others, we assigned annotation data to the analyzed cytokines from the OpenTargets database (59). OpenTargets compiles a global score for each protein, assessing its validity as a drug target, based on a collection of evidence from multiple data sources and modalities, such as genetic associations, somatic mutations, and RNA expression. In general, there was a moderate positive correlation between the global score in OpenTargets and the degree of cytokines in the UC naive network, indicating that the local importance of cytokines captured by the networks correlates with their candidacy as drugs ($R=0.44$, $P < 1.9e-06$, fig. S6). We also examined the OpenTargets score in the context of cytokine networks analyzed in this study (Fig. 6A). Based on the global score measure of OpenTargets, TL1A was the highest-scoring cytokine target in UC without an approved inhibitor drug. TL1A is a regulatory cytokine and susceptibility variant in IBD (60–62). It regulates important proinflammatory cytokines, such as TNF, IFN-γ, IL-17A, CSF2, IL-6, and IL-13 (63), most of which TL1A targets directly in the inflamed naive UC cytokine networks. Furthermore, TL1A was also one of the top rewired nodes between the cytokine networks, indicating that its interactome is significantly different across states (Fig. 3B). We plotted the $\log_2$ ratio of edge weights and Jaccard indexes of the cytokine-cytokine interactions compared to the healthy condition (Fig. 6C). To quantify the weight of cytokine-cytokine interactions, we used the number

of cell types participating in each cytokine-cytokine interaction. The upper right quadrant shows the interactions that not only have low Jaccard scores (dissimilar cell types participating in the interaction) but are also expanded in the UC treatment-naive condition (log_2 ratio > 2), indicating that a greater number and variety of cell types signal through TL1A compared to health. In the inflamed treatment-naive network, the TL1A-TGFB1 interaction had one of the lowest Jaccard scores and highest log_2 edge weight values across all of the interactions when compared to the healthy condition, indicating a marked shift in the composition and number of contributing cell types, involving inflammatory fibroblasts and reticular fibroblasts in the inflamed UC condition. Because TL1A is also implicated in fibrosis in IBD (64), this interaction reveals one of the potential mechanisms through which this becomes possible. We examined the specific differences in the participating cell types of the TL1A-TNF interaction between healthy controls and inflamed treatment-naive UC (Fig. 6D). Compared to the healthy state, in the inflamed treatment-naive condition, there was a substantial expansion in the putative immune cell types that are likely to respond to TL1A to produce TNF, including various $CD4^+$ and $CD8^+$ T cell subtypes, epithelial cell subtypes, including Goblet cells, $BEST4^+$ cells, and Tuft cells, and endothelial cells. TL1A sends the highest weight interactions to TNF compared to all of the other incoming TNF interactions, indicating the inclusion of additional cell types that produce TNF in response to the TL1A signal.

We also note that TL1A and three of its directly regulated cytokines (CSF2, IL-10, and IL-17A) all target TNF with expanded and disease-specific interactions compared to the healthy condition (Fig. 6, E and F). TL1A may affect the other important UC drug target, IL-23A, through a UC-specific interaction with IL-17A (Fig. 6, E and F). The anti-TL1A drug PF-06480605 has entered

a phase II drug trial (TUSCANY) in UC with positive results (65). The trial demonstrated a significant reduction in TNF, IL-23A, and other cytokines (including, IL-1β, IFN-γ, and CCL20) compared to baseline and a reduction in the activity of T_H17 cells and fibrosis pathways. The inhibited cytokine TL1A holds an upstream position in the inflamed treatment-naive network in relation to all cytokines found to be significantly reduced compared to baseline (Fig. 6F), as shown previously (65), capturing the potential mechanism through which this regulatory effect occurs, involving a number of UC-specific interactions.

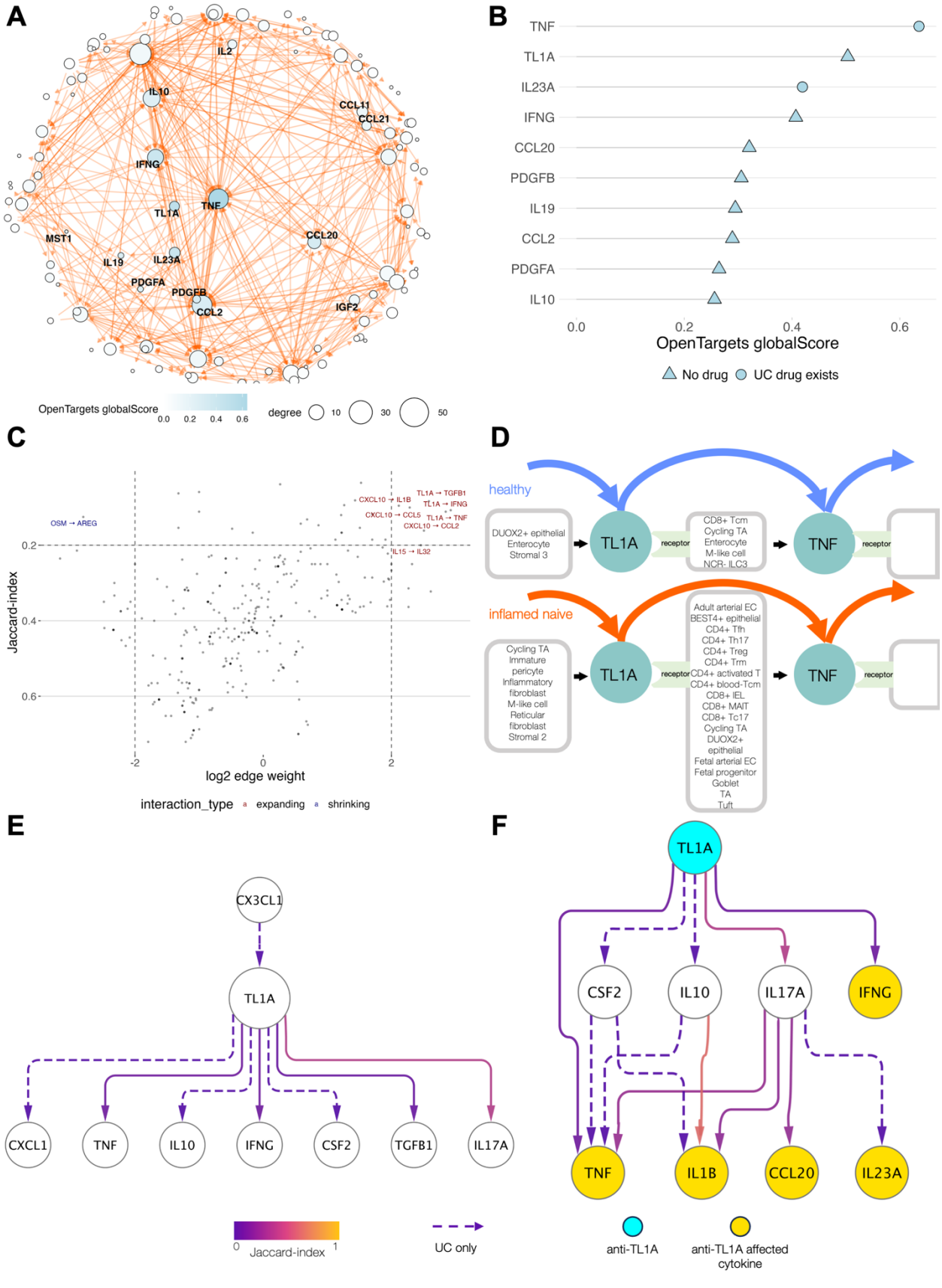
A
IL2
IL10
CCL11
CCL21
IFNG
TNF
TL1A
MST1
IL19
IL23A
CCL20
PDGFA
PDGFB
CCL2
IGF2
OpenTargets globalScore
0.0 0.2 0.4 0.6
degree 10 30 50
B
TNF
TL1A
IL23A
IFNG
CCL20
PDGFB
IL19
CCL2
PDGFA
IL10
0.0 0.2 0.4 0.6
OpenTargets globalScore
No drug
UC drug exists
C
OSM → AREG
CXCL10 → IL1B
TL1A → TGFB1
TL1A → IFNG
CXCL10 → CCL5
TL1A → TNF
CXCL10 → CCL2
IL15 → IL32
Jaccard-index
0.2
0.4
0.6
-2 0 2
log2 edge weight
interaction_type expanding shrinking
D
healthy
DUOX2+ epithelial
Enterocyte
Stromal 3
TL1A
receptor
CD8+ Tcm
Cycling TA
Enterocyte
M-like cell
NCR- ILC3
TNF
receptor
inflamed naive
Cycling TA
Immature
pericyte
Inflammatory
fibroblast
M-like cell
Reticular
fibroblast
Stromal 2
TL1A
receptor
Adult arterial EC
BEST4+ epithelial
CD4+ Tfh
CD4+ Th17
CD4+ Treg
CD4+ Trm
CD4+ activated T
CD4+ blood-Tcm
CD8+ IEL
CD8+ MAIT
CD8+ Tc17
Cycling TA
DUOX2+
epithelial
Fetal arterial EC
Fetal progenitor
Goblet
TA
Tuft
TNF
receptor
E
CX3CL1
TL1A
CXCL1
TNF
IL10
IFNG
CSF2
TGFB1
IL17A
0 Jaccard-index 1
UC only
F
TL1A
CSF2
IL10
IL17A
IFNG
TNF
IL1B
CCL20
IL23A
anti-TL1A
anti-TL1A affected cytokine

Figure 6. TL1A as a drug target in the treatment-naive cytokine network. A: UC inflamed treatment-naive cytokine network with the OpenTargets global score overlaid on the cytokines. **B**: Highest OpenTargets global score of cytokines, and available UC drugs. **C**: Scatterplot of log2 edge weight compared to health and Jaccard index of cell type similarity compared to health. Upper right quadrant indicates interactions that are simultaneously more expanded, and utilise different cell types compared to health. **D**: Cell types contributing to the expanded TL1A–TNF interaction. **E**: First neighbours of TL1A in the inflamed treatment-naive network. UC-specific interactions shown with dashed lines. **F**: Interactions from TL1A (blue) to all significantly affected cytokines in anti-TL1A treatment as shown in (65).

DISCUSSION

The complex network of interactions formed by cytokines is an important mechanism regulating immune responses in inflammatory diseases (66). However, the redundant and pleiotropic effects that cytokines exert on their target cells make it difficult to disentangle their respective roles (67, 68). Here, we constructed a systems biology model to resolve this by comprehensively collating all active cytokine-cytokine interactions in the system, capturing both the redundant and cell type–specific effects cytokines that may have on each other. We demonstrated the ability of this systems immunology model to capture physiologically relevant cytokine-cytokine interactions in both epithelial and immune cell compartments, both on an RNA and a protein level. This was achieved through a combination of approaches, including cross-referencing with a large, independent compendium of experimentally validated cytokine-cytokine interactions in murine immune cells (23), cytokine exposure experiments with colonic epithelial organoids derived from both healthy individuals and patients with UC, and organoid co-culture systems involving healthy human ILC1s and epithelial cells, enabling the prediction of cytokine targets driven by endogenous cytokine production.

We next sought to gain deeper insights into the cytokine networks underpinning UC, the prototypical chronic IMID, across different states based on inflammatory status and treatment

exposure. A better understanding of cytokine networks in IMIDs such as UC and how they alter according to inflammatory status or treatment will be critical for finding alternative, and more effective, therapeutic strategies (9, 69). In UC, the long-term remission rate of therapeutic agents, including anti-TNF and anti-p40 drugs, remains suboptimal at about 20 to 30% compared to placebo, imposing a "therapeutic ceiling" (13). For patient cohorts that do not respond well or become resistant to such advanced therapies, finding the cytokine signaling events that differ from responders or offer alternative intervention points could help inform strategies for overcoming this therapeutic ceiling in the future.

Our systems biology modelling revealed insights into the cytokine networks underpinning UC. We found a large cytokine subnetwork comprising cytokine-cytokine interactions that were specific to treatment-naive inflamed tissues. In this subnetwork, the cytokines with the greatest number of incoming interactions included TNF, IL-1β, IL-6, and CCL2, whereas IL-1α and resistin had the largest number of outgoing interactions. Rewiring analysis of cytokine networks pinpointed cytokines with the most altered interactions across disease states, revealing how treatment and inflammation status can alter cytokine signaling. The most rewired cytokines included IL-22, TL1A, IL-23A, and OSM. We found that TL1A is likely to function as an upstream regulator of key cytokines, including TNF and IL-23A, which are already pharmaceutically targeted in UC. Furthermore, many of the cytokines regulated by TL1A involve an increasing number of cell types, including $CD4^+$ and $CD8^+$ T cells, epithelial cells, and endothelial cells in the inflamed UC state compared to the healthy state. We also observed a putative pro-fibrotic signal mediated by TL1A through the activation of inflammatory and reticular fibroblasts resulting in TGFB1 release. Furthermore, TL1A emerged as one of the top druggable cytokine targets in our analysis based on

data from OpenTargets. This finding is consistent with results from phase II drug trials in UC targeting TL1A (TUSCANY), which demonstrated reduced expression of genes encoding TNF and IL-23A, and other cytokines (IL1B, IFNG, CCL20) captured downstream of TL1A by our model, as well as the alleviation of fibrosis and inflammation in patients after TL1A inhibition (65). Our analysis highlighted multiple other examples where the effect of a cytokine on its downstream targets was also identified in independent studies, such as the effect of IL-22 on its target CXC-chemokines (30), the induction of IL22 by IL-23A (42), and the targeting of IL-6 by OSM (14). Finally, by mapping the JAK paralog specificity of cytokine-cytokine interactions, including a module involving treatment-resistance genes (OSM and IL22) within the JAK1 signaling network, we revealed a possible mechanistic basis for the consistent efficacy of JAK inhibitors observed in both biologic naive patients and patients who previously failed biologics (57, 58).

The presented systems immunology modelling of cytokine-cytokine interactions enabled us to gain unique insights into UC pathogenesis. Other systems-level models capturing cytokine signaling are rare and tend to answer different questions from those that we proposed in our current study. Databases such as ImmuneXpresso and Immunoglobe (70, 71) collate a large amount of cell-cytokine or cytokine-cell interactions compiled from the literature, but do not consider direct cytokine-cytokine interactions, which were the primary focus of our analyses. Another study proposes a method to analyze the effects of the blockage of single cytokines on the secretion rate of target cytokines in IMIDs (20). The approach outlined in that study is a complementary modelling technique that could be combined with our systems-level method to identify the effects on putative intervention targets in the future.

Although our analysis captured physiologically relevant cytokine-cytokine interactions and yielded relevant findings, it is important to note that the presented study has several limitations that must be considered when contextualizing the results. The primary focus of our research was to study how cytokines affect each other and observe the rewiring of cytokine signaling in disease. Naturally, cytokines regulate non-cytokine target genes as well, which are not captured in our model, reducing the scope in which the interactions can be interpreted. On the other hand, we used a broad definition of cytokines that includes interleukins, chemokines, growth factors, and other factors to capture a more complete, yet potentially less focused, picture of immune signaling. In a complex condition such as UC, where inflammation and wound healing may be constitutively active, we decided on this broad definition to capture a more holistic overview of the underlying pathological mechanisms driven by cytokines (72). Furthermore, we modelled the individual cytokine-cytokine interactions as direct 1:1 relationships without considering their synergies, an important feature of cytokine regulation (73). However, such synergistic signaling interactions are computationally challenging to model, given the lack of comprehensive experimental work that has evaluated multiple cytokines individually and at the same time to delineate such relationships. Another challenge was the limited resolution of clinical metadata that was publicly available, hindering our ability to identify cytokine signaling changes modulated by specific immunomodulators or advanced therapies. In addition, the interactions can falter on multiple levels in all scRNA-seq studies focusing on intercellular communication (74). The sequenced RNAs in the scIBD datasets might not all be translated to generate proteins, the proteins made may not all be secreted, those that are secreted may not diffuse to the target cells, and those that do may not cause a response (75). Furthermore, cytokine signaling often occurs at both autocrine and paracrine

levels (76), requiring spatial information that is not captured with scRNA-seq data. In our model, we found that more two-thirds of the predicted interactions involved at least one shared cell type producing the primary and secondary cytokines (fig. S7), indicating that most cytokine signaling occurs at least at a partially autocrine level. However, with the increasing availability of spatial transcriptomics platforms, there is exciting potential for this limitation to be overcome (77–80).

In the future, more focused studies will be required to further disentangle the hierarchical and signed (stimulatory or inhibitory) nature of cytokine-cytokine interactions. Patient-derived organoid models provide a disease-specific genetic background (81), can be co-cultured with certain immune cell populations, and serve as a scalable in vitro model system that can be challenged with multiple compounds (82, 83). Appropriate time-series experiments could disentangle whether the cytokine-cytokine interactions are directly caused by the addition of an "upstream" cytokine or by second- or third-order effects. Although the method discussed in this work uses scRNA-seq data as its input, alternative methods exist that could be repurposed for cytokine-cytokine interaction inference using less expensive bulk transcriptomics data (84), paving the way to a much larger repository of publicly available datasets. Whereas more targeted validation is needed to confirm the directionality and stimulatory or inhibitory nature of the predicted cytokine-cytokine interactions, the ability to organize cytokine communication in relevant hierarchies could be harnessed to indicate future upstream targets, if direct intervention would not be available or desirable.

In conclusion, using our systems biology approach, we mapped the network of cytokine-cytokine interactions underpinning UC, revealing distinct interactions according to inflammatory state and

treatment exposure. We identified key rewired cytokines across disease states, a subnetwork of cytokine-cytokine interactions in inflamed colonic mucosa unique to treatment-naive UC patients, and pinpointed the putative JAK paralog proteins participating in each cytokine-cytokine interaction. Our analysis highlighted TL1A as an important upstream regulator of TNF, IL-23A, and other cytokines, and a potential driver of pro-fibrotic signaling in UC. Thus, our systems immunology modelling reveals insights that have the potential to inform the development of novel therapeutic strategies in UC. Although this study specifically focused on cytokine signaling in UC, our approach can be used to interrogate cytokine signaling in other inflammatory or infectious diseases to better understand how cytokine interactions contribute to the pathological mechanisms of disease.

MATERIALS AND METHODS

Data processing

Integrated, pre-processed scRNA-seq gene expression data was downloaded from scibd.cn (21) in .rds format. Data were read and processed with the Seurat (85) (version: 4.3) and tidyseurat (86) packages (version: 0.6). Samples were separated by disease condition (that is, UC, healthy) and status (inflamed, noninflamed) using the annotation provided by scIBD. Samples annotated as adult tissue biopsies were used for the generation of cytokine networks. In addition to the original disease conditions provided by the scIBD metadata, we generated an additional "UC inflamed naive" condition in the UC dataset. Using the supplementary information from the studies included in scIBD, in which patient treatment data were assigned to individual samples (rather than on a cohort level). Seven samples [studies: (2) Kinchen et al. (87), (3) Parikh et al. (88), (2) Corridoni et al. (89), sample identifiers: 'GSM3214201_A3', 'GSM3214204_B3', 'GSM3214207_C3',

'GSM4483695_S24','GSM4483696_S33','GSM3140595_UC1','GSM3140596_UC2') in UC did not receive any immunomodulatory or biologics treatment, and thus were considered treatment naive. Subsequently, these patients were removed from the “UC inflamed” category, which we then termed “UC inflamed treated.” We attempted to generate similar subclasses for the ‘UC noninflamed’ condition, but in that case, only three patients could be assigned to the “UC noninflamed naive” condition, which due to its small size was not comparable with the rest of the data. However, these three patients were excluded from the ‘UC noninflamed treated’ condition to achieve a more consistent output.

Construction of cytokine-cytokine networks

We used the R package NicheNet (prior model v2) to establish the cytokine-cytokine networks in IBD for each disease condition (healthy, UC: inflamed naive, inflamed treated, noninflamed treated) (22). The Seurat identity classes of the scIBD object were set to “minor_cluster”, containing the established cell types in the dataset. The gene set of interest was determined as all cytokines that were considered as such in the systems immunology databases ImmunoGlobe and ImmuneXpresso (70, 71) (table S1). The ligand activity analysis of NicheNet was performed for each cell type, querying cytokine ligands, indicating their potential in regulating their target gene sets of interest (downstream cytokines). Ligands were considered active if they achieved a Pearson correlation value > 0.1. The top-predicted target genes of the active cytokine ligands were established with the target prediction evaluation protocol in NicheNet, a multi-ligand random forest model with k-fold cross-validation (k = 5). Target downstream cytokines from the gene set of interest were kept if they were predicted in every cross-validation round.

Edge weights

To quantify the weight of the cytokine-cytokine interactions we used the number of cell type interactions participating in each cytokine-cytokine interaction. Individual cytokine-cytokine interactions were constructed by connecting cytokine-producing cell types with NicheNet that could plausibly influence each other's activity. In general terms: cell1 → cytokine1 → cell2 → cytokine2. Specific examples are as follows. A: Inflammatory monocyte → IL-1β → $CD8^+$ T cell → IL-4; this is an example of a IL-1β → IL-4 cytokine-cytokine interaction. B: Inflammatory monocyte → IL-1β → $CD16^+$ NK cell → IL-4: this is an example of a different IL-1β → IL4 cytokine-cytokine interaction, for which the site of IL-4 production differs. For this example, the edge weight for IL-1β → IL4 would be two, because two combinations of cell types provide the cytokine-cytokine interaction in this case. To better highlight differences between the edge weights compared to healthy, we calculated their log2 ratios compared to the healthy condition, for example, log2FC_IL1B_IL4_inflamed_naive = log2(IL1B-IL4_inflamed_naive/IL1B-IL4_healthy).

Network rewiring

The Cytoscape (version 3.9.1) (90) app DyNet (version 1.0) (40) was used to calculate the rewiring values between the network states, using the multiple comparison mode.

Network characteristics

The global and local importance of cytokine nodes in the networks was calculated with the tidygraph package (version 1.2.3), using the centrality_degree and centrality_betweenness functions. For the hierarchical clustering of networks, the dissimilarity matrix was calculated from

the adjacency matrices of the networks with the dist function in R, using the "euclidean" method. Clustering was performed using the hclust function, with the method set to "complete." The resulting object was written to a newick file with the ape package (91) was and visualized with the iTOL web service (92).

Cytokine paths

To find the shortest paths between queried source and target nodes, we used the PathLinker (93) Cytoscape application, with default settings.

Anti-TL1A affected cytokines

We used the results from Fig. 2B of the study by Hassan-Zahraee *et al*. (65) to collect the list of cytokine genes whose expression was significantly decreased after anti-TL1A treatment compared to baseline (IL1B, IL23A, CCL20, IFNG, and TNF).

JAK specificity of cytokine–cytokine interactions

We used the get_ligand_signaling_path function from NicheNet to query the intracellular nodes in each cell type used by each cytokine-cytokine interaction, with the "top_n_regulators" argument set to 10, and the NicheNet-weighted network filtered to contain only expressed genes. For each cytokine-cytokine interaction, the JAK proteins involved in the signaling pathways were recorded. To assess the precision of the affected interactions, we compared the number of correct and incorrect JAK usages for nine cytokines for which their JAK preferences are known and their downstream targets are found in the network (11).

Open Targets global score

The OpenTargets global score was downloaded by querying “ulcerative colitis” (EFO_0000729) on the Open Targets Platform (https://platform.opentargets.org/) (accessed 01/02/2024). The results were exported as a .tsv file, and the resulting hits were filtered to only contain cytokine genes present in our study. For the calculation of the global score and source data weights please refer to https://platform-docs.opentargets.org/associations. Correlation with degree was calculated with the stat_cor function of the ggpubr package (version 0.6.0).

Three-dimensional (3D) colonic organoid culture

Four human organoid lines from the Imperial BRC Organoid biobank were used in this study. These lines were generated from rectal or sigmoid colon tissue from patients with quiescent to mild UC (2 women and 2 men between 30 and 72 years of age). Derived organoid lines were cultured as 3D structures embedded in Matrigel ExtraCellular Matrix, (Corning, Growth Factor Reduced Cat # 356231) diluted with Advanced DMEM/F12 medium using a 4:1 ratio (Thermofisher Scientific, Cat # 12634) in Corning 3527 24-well plates (VWR International Gmbh, Cat # 734-1605). Organoids were expanded and fed every other day with complete Intesticult Organoid Growth Medium (OGM, Human, StemCell Technologies, Cat # 06010), supplemented with 10 μM Rho Kinase inhibitor Y-27632 (Tocris, Cat # 1254) and 100 μg/ml Primocin (Invivogen, Cat # ant-pm-1) at 37°C, 5% CO_2 in a humidified incubator. Organoids were then differentiated in complete Intesticult Organoid Differentiation Medium (ODM, Human, StemCell Technologies, Cat # 100-0214) supplemented with 10 μM γ-secretase inhibitor (DAPT) (Biotechne Ltd, Cat #2634/10) and 100 μg/ml Primocin. Differentiation was performed at 37°C, 5% CO_2 in a humidified incubator. Organoids were cultured for 4 days before any treatment.

Colonic organoid IFN-γ treatments

The inflammatory status of the differentiated UC patient organoids was regained through a 24-hour treatment with a cocktail containing 100 ng/ml TNFα (Invivogen, Cat # rcyc-htnfa), 20 ng/ml IL-1β (Peproteck, UK, Cat # 200-1B) and 100 ng/ml Flagellin (Invivogen, Cat # tlrl-fliC-10) in complete ODM containing 10 μM DAPT and 100 μg/ml Primocin. When required, 100 ng/ml IFNγ (Thermo Fisher Scientific (Hemel), Cat # PHC4031) was added to the medium concomitantly or not to the inflammatory cocktail for the 24-hour incubation before the experimental end point. At the end of the experiment, the potential cytotoxicity of the conditioned medium was tested on an aliquot of medium collected from each technical replicate with the CytoTox 96 Non-Radioactive Cytotoxicity Assay kit (Promega, Cat # G1780). Each condition was tested in 8 technical replicates for each organoid line (biological replicates).

RNA extraction

At the end of the experiment, each colonic organoid-containing Matrigel dome was rinsed with pre-warmed DPBS (Merck, Cat # D8537). For each condition, the organoids were harvested in cell recovery solution (Corning®, Cat # 354253), technical replicates were pooled two by two to ensure enough material was obtained for RNA subtraction. Organoids were then spun down at 300*g* at 4°C for 5 min and immediately lysed in the β-mercaptoethanol–containing lysis solution with the RNeasy minikit (Qiagen Cat # 74104). RNA was extracted according to the manufacturer's instructions and eluted in 10 mM Tris-HCl, pH 8. All samples with an RIN >=7 were used for sequencing.

Library preparation and sequencing

The libraries for this study were constructed by the Technical Genomics Team at the Earlham Institute, Norwich, UK, using the NEBNext Ultra II RNA Library prep for Illumina kit (NEB#E7760L), NEBNext Poly(A) mRNA Magnetic Isolation Module (NEB#E7490L), and NEBNext Multiplex Oligos for Illumina (96 Unique Dual Index Primer Pairs) (E6440S/L) at a concentration of 10 μM. Library preparation was performed on a Perkin Elmer (formerly Caliper LS) Sciclone G3 (PerkinElmer PN: CLS145321). RNA (1 μg) was purified to extract mRNA with a Poly(A) mRNA Magnetic Isolation Module. The technology is based on the coupling of Oligo d(T)25 to paramagnetic beads, which facilitates the binding of poly(A)+ RNA. Isolated mRNA was then fragmented for 12 min at 94°C, and first-strand cDNA was synthesized. This process reverse-transcribes the RNA fragments primed with random hexamers into first-strand cDNA using reverse transcriptase and random primers. The second strand synthesis process removes the RNA template and synthesizes a replacement strand to generate double-stranded cDNA. Directionality was retained by adding dUTP during the second strand synthesis step and subsequent cleavage of the uridine-containing strand with USER Enzyme (a combination of UDG and Endo VIII). NEBNext Adaptors were ligated to end-repaired, dA-tailed DNA. The NEBNext Adaptors with novel hairpin loop structure are designed to ligate with high efficiency and minimize adaptor-dimer formation. The loop contains a U, which is removed by treatment with USER Enzyme to open the loop and make it available as a substrate for PCR. The ligated products were subjected to a bead-based purification with Beckman Coulter AMPure XP beads (A63882) to remove most of the un-ligated adaptors. Adaptor Ligated DNA was then enriched by receiving 10 cycles of PCR (30 s at 98°C, 10 cycles of: 10 s at 98°C, 75 s at 65°C, and 5 min at 65°C, with a final hold at 4°C). Barcodes were incorporated during PCR with NEBNext Multiplex Oligos for

Illumina (96 Unique Dual Index Primer Pairs) thereby enabling multiplexing. The size of the libraries was estimated with the Perkin Elmer GX Touch DNA High Sensitivity assay (DNA High Sensitivity Reagent Kit CLS760672), and the concentrations were quantified by fluorescence, with a high-sensitivity plate reader Quant-iT dsDNA Assay Kit, (ThermoFisher Q-33120). The resulting libraries were then equimolarly pooled, and q-PCR was performed on the pool before sequencing. The pool was sequenced on one lane of an Illumina NovaSeq 6000 S4 flow cell with 150-bp paired-end reads.

Bulk RNA-seq processing

Bulk RNA-seq data was preprocessed by our in-house TranscriptOmiX pipeline (https://github.com/korcsmarosgroup/Transcriptomix). The pipeline is made up of the following steps: Pre-alignment Quality Control (FastQC (version v0.12.0) (94), generating genome index [STAR (version 2.7.10a) genomeGenerate with sjdbOverhang 99, using GRCh38.108 genome annotations], Alignment (STAR alignment) (95), Quantification [featureCounts (version 1.22.2)] (96), Post Alignment Quality control [MultiQC (version 1.14)] (97). Differential expression analysis was performed on normalized counts by DESeq2 (version 1.34.0) (98) (padj_cutoff = 0.05, alpha = 0.05) with lfcShrink, comparing all pairwise conditions.

Tissue-derived human small intestinal organoid generation, maintenance, and maturation

Tissue-derived human small intestinal organoids (hSIOs) were established according to a previously published protocol (99). The cultures were passaged every 7 to 10 days by enzymatic dissociation with TryplE (12604013, Thermofisher). The cells were then spun down, resuspended

in Matrigel (Corning), and fed with complete Organoid Growth Medium (STEMCELL Technologies) (table S3).

ILC1 maturation from innate lymphoid cell precursors and co-culture with iPSC-derived human small intestinal organoids

ILC1s were matured and expanded from innate lymphoid cell precursors (ILCPs). ILCPs were isolated with a BD FACS ARIA II/III based on the following markers: $CD45^+$, Lineage (CD14, CD19, CD20, CD3, TCRαβ, TCRγδ)$^-$, $CD127^+$, $KLRG1^-$, $CD4^-$, $NKp46^-$, $CD56^-$, $CRTH2^-$, and $cKIT^+$. ILCPs were co-cultured with iPSC-derived human intestinal organoids (HIO) in ILCP expansion medium for 14 days, according to previous protocols (100, 101) to differentiate them into intestinal-like ILC1s (fig. S8). KUTE-4 iPSCs were previously generated (102) and maintained on tissue culture plates coated with Vitronectin (StemCell Technologies) in Essential 8 medium (Gibco). iPSCs were passaged as disrupted clusters every 4 to 7 days with Versene (Gibco) with 10 μM Y-27632 (a Rho kinase inhibitor; TOCRIS) added for the first 24 hours after passaging. iPSC-derived human intestinal organoids (HIOs) were generated according to previously established protocols (103, 104), with substitution of recombinant Wnt3a (105) for the GSK3 inhibitor CHIR99021 and the addition of IL-2 (2 ng/ml) to the HIO maturation medium (table S3) (106) for further maturation. HIOs were passaged and reseeded in Matrigel every 8 to 14 days. HIOs were matured for at least 4 weeks in HIO maturation medium before use in experiments.

ILC1 and hSIO co-culture set-up

Five days before the co-culture was established, hSIOs were fed with complete Organoid Differentiation Medium (STEMCELL Technologies) (table S4) to induce stem cell differentiation into mature intestinal cells. On the first day of co-culture, hSIOs were harvested, spun down and counted. Approximately 150 to 200 organoids were combined with 2 x 10^4 FACS-purified ILC1s ($CD45^+$, Lineage (CD14, CD19, CD20, CD3, TCRαβ, TCRγδ)$^-$, $CD4^-$, $CRTH2^-$, $cKIT^-$, $CD56^-$, $CD161^+$) per well before centrifugation at 300g for 5 min and resuspension in Matrigel. For hSIO-only controls, 150 to 200 hSIOs were also plated in monocultures. Both ILC1-hSIO co-cultures and hSIO monocultures were maintained in 500 µl of human co-culture medium (tableS4) for 5 days. Each day, 100 µl of medium was removed from the cultures and stored at -80°C for subsequent analysis, and an additional 150 µl of human co-culture medium was added on top of the cultures.

Cytokine analysis from co-culture medium

Cytokine concentrations in co-culture medium were quantified by LEGENDplex Mix-and-Match-Panel bead assays (BioLegend). The Human Proinflammatory Chemokine Panel LEGENDplex assay was used to detect CCL17, CCL5, CXCL11, CCL3, CXCL1, CCL20, and CXCL10 (#740991, #740992, #740997, #740993, #740996, #740995, #740989, respectively) in day-4 samples. The Human Neuroinflammation Panel 1 LEGENDplex assay was used to quantify the amounts of CCL2, IL-6, TNF-α, and β-NGF (#740793, #740800, #740803, #740802, respectively) in day-5 samples. Finally, the Human Cytokine Panel 2 LEGENDplex kit was used to measure the concentrations of IL-1β, GM-CSF, IL-18, and IL-1α (#741380, #740106, #741382, #740104, respectively) in day-3 samples. Culture medium (25 µl) was applied neat and in 1:10 dilution in assay buffer for the measurements. The LEGENDplex assays were performed according to the

manufacturer's instructions. A BD LSRFortessa instrument was used for flow cytometry analysis of the assay beads. To calculate the cytokine concentrations in the medium, we used the LEGENDplex software from BioLegend (https://legendplex.qognit.com).

Computational analyses to validate cytokine-cytokine interactions

To validate the physiological relevance of cytokine-cytokine interactions, we compared them to multiple experimental datasets. First, we downloaded the differential expression results of the Immune Dictionary study from Supplementary Table 3 of the study by Cui *et al*. (23), to compare cytokine responses in immune cell populations to upstream cytokines administered to mice models. Mouse gene identifiers were mapped to human symbols using the convert_mouse_to_human_symbols function in NicheNet. The significance of target set overlap and set similarity were determined between the Immune Dictionary results and all generated cytokine networks, where comparable source cytokines (that is, cytokines affecting other cytokines) were found. To calculate the significance of the overlap between cytokine target genes captured by the computational model and the experiments used for validation, for the Immune Dictionary results, we used the hypergeometric test from R (version 4.1.2) with the phyper function, with the argument lower.tail set to false. Multiple testing was corrected with the "fdr" method of the p.adjust function in R. The similarity of the input sets was measured with the Jaccard-index, calculated with a custom R function. To compare the computational results to the organoid experiments, the generated cytokine networks from the UC conditions were filtered to contain only interactions between epithelial cell types also present in colonic organoid models (Goblet, Enterocyte, Cycling TA, TA, Enteroendocrine, Adult colonocyte, Pediatric colonocyte, and BEST4+ epithelial). We compared the downstream cytokine targets of IFN-γ in these reduced

models with differentially expressed cytokine genes from bulk RNA-seq data from patient-derived UC colonic organoids treated with IFN-γ, as described earlier. To determine the enrichment of predicted IFN-γ target cytokines, we classified the target cytokines as a new gene set and used them as input for gene set enrichment analysis (GSEA) with the R library fgsea (version 1.32) (107). Results were visualized with enrichment plots and quantified using normalized enrichment scores (NES). When validating the healthy network, the same approach was used: cells were filtered to only contain interactions between epithelial cell types also present in colonic organoid models, and the downstream cytokine targets of TNF, IFN-γ, and IL-17A were assigned to their respective gene sets. Differential gene expression results from the study by Pavlidis *et al*. (29) were downloaded from GEO (Accession GSE190634) and processed using GEO2R with default settings. The GSEA of the TNF, IFN-γ, and IL-17A gene sets was executed as for the UC networks, using fgsea (version 1.32) with nperm set to 1000. For the analysis of co-cultured ILC1 cells and hSIOs, a reduced in silico model was generated as for the colonic organoids. Integrated scRNA-seq data from the original scIBD object were filtered for 'healthy' disease state and 'smallInt' tissue, and the resulting object was processed with the cytokine network pipeline as described earlier. To ascertain the downstream cytokine targets of TGFB1, IFNG, and TNF, the target cells in the resulting network were filtered in the same manner as for the colonic organoid models, only containing organoid-relevant epithelial cell types. We chose the 20 downstream targets of TGFB1, IFNG, and TNF that were shared by both the colonic and small-intestinal in silico model for experimental validation (CCL17, CCL2, CCL5, CSF1, CXCL10, CXCL11, IL1B, IL33, IL6, TNF, TNFSF13B, CCL3, CXCL1, NGF, PDGFA, WNT5A, CCL20, CSF2, CXCL3, and IL1A), 14 of which were included in the selected BioLegend assays. For the statistical analysis of the results, the LEGENDplex software output files were read into R, and the predicted concentration values

of co-culture and standalone organoid samples were tested using the Wilcoxon-Rank Sum test, and normality was tested using the Shapiro-Wilk test ('shapiro.test' in R). The results from the neat dilution experiments were used in the final analysis, and plots were generated with the ggpubr package (108).

Supplementary Materials
Figs. S1 to S8.
Tables S1 to S5.

References and Notes

1. M. J. Cameron, D. J. Kelvin, Cytokines, Chemokines and Their Receptors - Madame Curie Bioscience Database - NCBI Bookshelf (2013).
2. R. Morris, N. J. Kershaw, J. J. Babon, The molecular details of cytokine signaling via the JAK/STAT pathway. Protein Sci. 27, 1984–2009 (2018).
3. S. H. Chan, B. Perussia, J. W. Gupta, M. Kobayashi, M. Pospísil, H. A. Young, S. F. Wolf, D. Young, S. C. Clark, G. Trinchieri, Induction of interferon gamma production by natural killer cell stimulatory factor: characterization of the responder cells and synergy with other inducers. J. Exp. Med. 173, 869–879 (1991).
4. J. Ye, J. R. Ortaldo, K. Conlon, R. Winkler-Pickett, H. A. Young, Cellular and molecular mechanisms of IFN-gamma production induced by IL-2 and IL-12 in a human NK cell line. J. Leukoc. Biol. 58, 225–233 (1995).
5. J. H. Dufour, M. Dziejman, M. T. Liu, J. H. Leung, T. E. Lane, A. D. Luster, IFN-gamma-inducible protein 10 (IP-10; CXCL10)-deficient mice reveal a role for IP-10 in effector T cell generation and trafficking. J. Immunol. 168, 3195–3204 (2002).
6. M. Friedrich, M. Pohin, F. Powrie, Cytokine networks in the pathophysiology of inflammatory bowel disease. Immunity. 50, 992–1006 (2019).
7. S. C. Ng, H. Y. Shi, N. Hamidi, F. E. Underwood, W. Tang, E. I. Benchimol, R. Panaccione, S. Ghosh, J. C. Y. Wu, F. K. L. Chan, J. J. Y. Sung, G. G. Kaplan, Worldwide incidence and prevalence of inflammatory bowel disease in the 21st century: a systematic review of population-based studies. Lancet. 390, 2769–2778 (2017).
8. T. Kobayashi, B. Siegmund, C. Le Berre, S. C. Wei, M. Ferrante, B. Shen, C. N. Bernstein, S. Danese, L. Peyrin-Biroulet, T. Hibi, Ulcerative colitis. Nat. Rev. Dis. Primers. 6, 74 (2020).
9. T. Takeuchi, Cytokines and cytokine receptors as targets of immune-mediated inflammatory diseases-RA as a role model. Inflamm. Regen. 42, 35 (2022).
10. G. Schett, I. B. McInnes, M. F. Neurath, Reframing Immune-Mediated Inflammatory Diseases through Signature Cytokine Hubs. N. Engl. J. Med. 385, 628–639 (2021).
11. M. F. Neurath, Strategies for targeting cytokines in inflammatory bowel disease. Nat. Rev. Immunol. 24, 559–576 (2024).
12. M. F. Neurath, Current and emerging therapeutic targets for IBD. Nat. Rev. Gastroenterol. Hepatol. 14, 269–278 (2017).

13. D. Alsoud, B. Verstockt, C. Fiocchi, S. Vermeire, Breaking the therapeutic ceiling in drug development in ulcerative colitis. Lancet Gastroenterol. Hepatol. 6, 589–595 (2021).
14. N. R. West, A. N. Hegazy, B. M. J. Owens, S. J. Bullers, B. Linggi, S. Buonocore, M. Coccia, D. Görtz, S. This, K. Stockenhuber, J. Pott, M. Friedrich, G. Ryzhakov, F. Baribaud, C. Brodmerkel, C. Cieluch, N. Rahman, G. Müller-Newen, R. J. Owens, A. A. Kühl, F. Powrie, Oncostatin M drives intestinal inflammation and predicts response to tumor necrosis factor-neutralizing therapy in patients with inflammatory bowel disease. Nat. Med. 23, 579–589 (2017).
15. C. A. Lamb, A. Saifuddin, N. Powell, F. Rieder, The future of precision medicine to predict outcomes and control tissue remodeling in inflammatory bowel disease. Gastroenterology. 162, 1525–1542 (2022).
16. B. G. Feagan, B. E. Sands, W. J. Sandborn, M. Germinaro, M. Vetter, J. Shao, S. Sheng, J. Johanns, J. Panés, VEGA Study Group, Guselkumab plus golimumab combination therapy versus guselkumab or golimumab monotherapy in patients with ulcerative colitis (VEGA): a randomised, double-blind, controlled, phase 2, proof-of-concept trial. Lancet Gastroenterol. Hepatol. 8, 307–320 (2023).
17. G. Roda, M. Marocchi, A. Sartini, E. Roda, Cytokine networks in ulcerative colitis. Ulcers. 2011, 1–5 (2011).
18. M. Vebr, R. Pomahačová, J. Sýkora, J. Schwarz, A narrative review of cytokine networks: pathophysiological and therapeutic implications for inflammatory bowel disease pathogenesis. Biomedicines. 11 (2023), doi:10.3390/biomedicines11123229.
19. M. Olbei, J. P. Thomas, I. Hautefort, A. Treveil, B. Bohar, M. Madgwick, L. Gul, L. Csabai, D. Modos, T. Korcsmaros, CytokineLink: A Cytokine Communication Map to Analyse Immune Responses-Case Studies in Inflammatory Bowel Disease and COVID-19. Cells. 10 (2021), doi:10.3390/cells10092242.
20. J. E. Jansen, D. Aschenbrenner, H. H. Uhlig, M. C. Coles, E. A. Gaffney, A method for the inference of cytokine interaction networks. PLoS Comput. Biol. 18, e1010112 (2022).
21. H. Nie, P. Lin, Y. Zhang, Y. Wan, J. Li, C. Yin, L. Zhang, Single-cell meta-analysis of inflammatory bowel disease with scIBD. Nat. Comput. Sci. 3, 522–531 (2023).
22. R. Browaeys, W. Saelens, Y. Saeys, NicheNet: modeling intercellular communication by linking ligands to target genes. Nat. Methods. 17, 159–162 (2020).
23. A. Cui, T. Huang, S. Li, A. Ma, J. L. Pérez, C. Sander, D. B. Keskin, C. J. Wu, E. Fraenkel, N. Hacohen, Dictionary of immune responses to cytokines at single-cell resolution. Nature. 625, 377–384 (2024).
24. D. Masopust, C. P. Sivula, S. C. Jameson, Of mice, dirty mice, and men: using mice to understand human immunology. J. Immunol. 199, 383–388 (2017).
25. L. E. Wagar, R. M. DiFazio, M. M. Davis, Advanced model systems and tools for basic and translational human immunology. Genome Med. 10, 73 (2018).
26. J. Mestas, C. C. W. Hughes, Of mice and not men: differences between mouse and human immunology. J. Immunol. 172, 2731–2738 (2004).
27. K. Arnauts, B. Verstockt, A. S. Ramalho, S. Vermeire, C. Verfaillie, M. Ferrante, Ex vivo mimicking of inflammation in organoids derived from patients with ulcerative colitis. Gastroenterology. 159, 1564–1567 (2020).
28. V. Langer, E. Vivi, D. Regensburger, T. H. Winkler, M. J. Waldner, T. Rath, B. Schmid, L. Skottke, S. Lee, N. L. Jeon, T. Wohlfahrt, V. Kramer, P. Tripal, M. Schumann, S. Kersting, C. Handtrack, C. I. Geppert, K. Suchowski, R. H. Adams, C. Becker, M. Stürzl, IFN-γ drives

inflammatory bowel disease pathogenesis through VE-cadherin-directed vascular barrier disruption. J. Clin. Invest. 129, 4691–4707 (2019).
29. P. Pavlidis, A. Tsakmaki, A. Treveil, K. Li, D. Cozzetto, F. Yang, U. Niazi, B. H. Hayee, M. Saqi, J. Friedman, T. Korcsmaros, G. Bewick, N. Powell, Cytokine responsive networks in human colonic epithelial organoids unveil a molecular classification of inflammatory bowel disease. Cell Rep. 40, 111439 (2022).
30. P. Pavlidis, A. Tsakmaki, E. Pantazi, K. Li, D. Cozzetto, J. Digby-Bell, F. Yang, J. W. Lo, E. Alberts, A. C. C. Sa, U. Niazi, J. Friedman, A. K. Long, Y. Ding, C. D. Carey, C. Lamb, M. Saqi, M. Madgwick, L. Gul, A. Treveil, N. Powell, Interleukin-22 regulates neutrophil recruitment in ulcerative colitis and is associated with resistance to ustekinumab therapy. Nat. Commun. 13, 5820 (2022).
31. G. M. Jowett, M. D. A. Norman, T. T. L. Yu, P. Rosell Arévalo, D. Hoogland, S. T. Lust, E. Read, E. Hamrud, N. J. Walters, U. Niazi, M. W. H. Chung, D. Marciano, O. S. Omer, T. Zabinski, D. Danovi, G. M. Lord, J. Hilborn, N. D. Evans, C. A. Dreiss, L. Bozec, E. Gentleman, ILC1 drive intestinal epithelial and matrix remodelling. Nat. Mater. 20, 250–259 (2021).
32. R. L. R. E. Taggenbrock, K. P. J. M. van Gisbergen, ILC1: Development, maturation, and transcriptional regulation. Eur. J. Immunol. 53, e2149435 (2023).
33. N. C. Di Paolo, D. M. Shayakhmetov, Interleukin 1α and the inflammatory process. Nat. Immunol. 17, 906–913 (2016).
34. C. P. McEntee, C. M. Finlay, E. C. Lavelle, Divergent Roles for the IL-1 Family in Gastrointestinal Homeostasis and Inflammation. Front. Immunol. 10, 1266 (2019).
35. A. Konrad, M. Lehrke, V. Schachinger, F. Seibold, R. Stark, T. Ochsenkühn, K. G. Parhofer, B. Göke, U. C. Broedl, Resistin is an inflammatory marker of inflammatory bowel disease in humans. Eur. J. Gastroenterol. Hepatol. 19, 1070–1074 (2007).
36. N. Silswal, A. K. Singh, B. Aruna, S. Mukhopadhyay, S. Ghosh, N. Z. Ehtesham, Human resistin stimulates the pro-inflammatory cytokines TNF-alpha and IL-12 in macrophages by NF-kappaB-dependent pathway. Biochem. Biophys. Res. Commun. 334, 1092–1101 (2005).
37. C. Guo, K. Wu, X. Liang, Y. Liang, R. Li, Infliximab clinically treating ulcerative colitis: A systematic review and meta-analysis. Pharmacol. Res. 148, 104455 (2019).
38. A. Andoh, A. Nishida, Molecular basis of intestinal fibrosis in inflammatory bowel disease. Inflamm. Intest. Dis. 7, 119–127 (2023).
39. C. Eftychi, R. Schwarzer, K. Vlantis, L. Wachsmuth, M. Basic, P. Wagle, M. F. Neurath, C. Becker, A. Bleich, M. Pasparakis, Temporally Distinct Functions of the Cytokines IL-12 and IL-23 Drive Chronic Colon Inflammation in Response to Intestinal Barrier Impairment. Immunity. 51, 367-380.e4 (2019).
40. I. H. Goenawan, K. Bryan, D. J. Lynn, DyNet: visualization and analysis of dynamic molecular interaction networks. Bioinformatics. 32, 2713–2715 (2016).
41. C. A. Lindemans, M. Calafiore, A. M. Mertelsmann, M. H. O'Connor, J. A. Dudakov, R. R. Jenq, E. Velardi, L. F. Young, O. M. Smith, G. Lawrence, J. A. Ivanov, Y.-Y. Fu, S. Takashima, G. Hua, M. L. Martin, K. P. O'Rourke, Y.-H. Lo, M. Mokry, M. Romera-Hernandez, T. Cupedo, A. M. Hanash, Interleukin-22 promotes intestinal-stem-cell-mediated epithelial regeneration. Nature. 528, 560–564 (2015).
42. D. Bauché, B. Joyce-Shaikh, J. Fong, A. V. Villarino, K. S. Ku, R. Jain, Y.-C. Lee, L. Annamalai, J. H. Yearley, D. J. Cua, IL-23 and IL-2 activation of STAT5 is required for optimal IL-22 production in ILC3s during colitis. Sci. Immunol. 5 (2020), doi:10.1126/sciimmunol.aav1080.

43. S. Verstockt, B. Verstockt, K. Machiels, M. Vancamelbeke, M. Ferrante, I. Cleynen, G. De Hertogh, S. Vermeire, Oncostatin M is a biomarker of diagnosis, worse disease prognosis, and therapeutic nonresponse in inflammatory bowel disease. Inflamm. Bowel Dis. 27, 1564–1575 (2021).
44. X. Zhao, W. Yang, T. Yu, Y. Yu, X. Cui, Z. Zhou, H. Yang, Y. Yu, A. J. Bilotta, S. Yao, J. Xu, J. Zhou, G. S. Yochum, W. A. Koltun, A. Portolese, D. Zeng, J. Xie, I. V. Pinchuk, H. Zhang, Y. Cong, Th17 Cell-Derived Amphiregulin Promotes Colitis-Associated Intestinal Fibrosis Through Activation of mTOR and MEK in Intestinal Myofibroblasts. Gastroenterology. 164, 89–102 (2023).
45. M. Kurimoto, T. Watanabe, K. Kamata, K. Minaga, M. Kudo, IL-33 as a Critical Cytokine for Inflammation and Fibrosis in Inflammatory Bowel Diseases and Pancreatitis. Front. Physiol. 12, 781012 (2021).
46. M. A. Williams, A. O'Callaghan, S. C. Corr, IL-33 and IL-18 in Inflammatory Bowel Disease Etiology and Microbial Interactions. Front. Immunol. 10, 1091 (2019).
47. B. Siegmund, G. Fantuzzi, F. Rieder, F. Gamboni-Robertson, H. A. Lehr, G. Hartmann, C. A. Dinarello, S. Endres, A. Eigler, Neutralization of interleukin-18 reduces severity in murine colitis and intestinal IFN-gamma and TNF-alpha production. Am. J. Physiol. Regul. Integr. Comp. Physiol. 281, R1264-73 (2001).
48. D. Polosukhina, K. Singh, M. Asim, D. P. Barry, M. M. Allaman, D. M. Hardbower, M. B. Piazuelo, M. K. Washington, A. P. Gobert, K. T. Wilson, L. A. Coburn, CCL11 exacerbates colitis and inflammation-associated colon tumorigenesis. Oncogene. 40, 6540–6546 (2021).
49. T. Castro-Dopico, A. Fleming, T. W. Dennison, J. R. Ferdinand, K. Harcourt, B. J. Stewart, Z. Cader, Z. K. Tuong, C. Jing, L. S. C. Lok, R. J. Mathews, A. Portet, A. Kaser, S. Clare, M. R. Clatworthy, GM-CSF Calibrates Macrophage Defense and Wound Healing Programs during Intestinal Infection and Inflammation. Cell Rep. 32, 107857 (2020).
50. E. Landy, H. Carol, A. Ring, S. Canna, Biological and clinical roles of IL-18 in inflammatory diseases. Nat. Rev. Rheumatol. 20, 33–47 (2024).
51. L. Chen, X.-L. Zhong, W.-Y. Cao, M.-L. Mao, D.-D. Liu, W.-J. Liu, X.-Y. Zu, J.-H. Liu, IGF2/IGF2R/Sting signaling as a therapeutic target in DSS-induced ulcerative colitis. Eur. J. Pharmacol. 960, 176122 (2023).
52. Z. Xie, G. Zhou, M. Zhang, J. Han, Y. Wang, X. Li, Q. Wu, M. Li, S. Zhang, Recent developments on BMPs and their antagonists in inflammatory bowel diseases. Cell Death Discov. 9, 210 (2023).
53. M. Sochal, M. Ditmer, A. Gabryelska, P. Białasiewicz, The Role of Brain-Derived Neurotrophic Factor in Immune-Related Diseases: A Narrative Review. J. Clin. Med. 11 (2022), doi:10.3390/jcm11206023.
54. R. Hjortebjerg, K. L. Thomsen, J. Agnholt, J. Frystyk, The IGF system in patients with inflammatory bowel disease treated with prednisolone or infliximab: potential role of the stanniocalcin-2 / PAPP-A / IGFBP-4 axis. BMC Gastroenterol. 19, 83 (2019).
55. X. Hu, J. Li, M. Fu, X. Zhao, W. Wang, The JAK/STAT signaling pathway: from bench to clinic. Signal Transduct. Target. Ther. 6, 402 (2021).
56. S. Honap, A. Agorogianni, M. J. Colwill, S. K. Mehta, F. Donovan, R. Pollok, A. Poullis, K. Patel, JAK inhibitors for inflammatory bowel disease: recent advances. Frontline Gastroenterol. 15, 59–69 (2024).
57. W. J. Sandborn, C. Su, B. E. Sands, G. R. D'Haens, S. Vermeire, S. Schreiber, S. Danese, B. G. Feagan, W. Reinisch, W. Niezychowski, G. Friedman, N. Lawendy, D. Yu, D. Woodworth,

A. Mukherjee, H. Zhang, P. Healey, J. Panés, OCTAVE Induction 1, OCTAVE Induction 2, and OCTAVE Sustain Investigators, Tofacitinib as induction and maintenance therapy for ulcerative colitis. N. Engl. J. Med. 376, 1723–1736 (2017).
58. S. Danese, S. Vermeire, W. Zhou, A. L. Pangan, J. Siffledeen, S. Greenbloom, X. Hébuterne, G. D'Haens, H. Nakase, J. Panés, P. D. R. Higgins, P. Juillerat, J. O. Lindsay, E. V. Loftus, W. J. Sandborn, W. Reinisch, M.-H. Chen, Y. Sanchez Gonzalez, B. Huang, W. Xie, R. Panaccione, Upadacitinib as induction and maintenance therapy for moderately to severely active ulcerative colitis: results from three phase 3, multicentre, double-blind, randomised trials. Lancet. 399, 2113–2128 (2022).
59. D. Ochoa, A. Hercules, M. Carmona, D. Suveges, J. Baker, C. Malangone, I. Lopez, A. Miranda, C. Cruz-Castillo, L. Fumis, M. Bernal-Llinares, K. Tsukanov, H. Cornu, K. Tsirigos, O. Razuvayevskaya, A. Buniello, J. Schwartzentruber, M. Karim, B. Ariano, R. E. Martinez Osorio, E. M. McDonagh, The next-generation Open Targets Platform: reimagined, redesigned, rebuilt. Nucleic Acids Res. 51, D1353–D1359 (2023).
60. R. Thiébaut, S. Kotti, C. Jung, F. Merlin, J. F. Colombel, M. Lemann, S. Almer, C. Tysk, M. O'Morain, M. Gassull, V. Binder, Y. Finkel, L. Pascoe, J. P. Hugot, TNFSF15 polymorphisms are associated with susceptibility to inflammatory bowel disease in a new European cohort. Am. J. Gastroenterol. 104, 384–391 (2009).
61. F. Furfaro, L. Alfarone, D. Gilardi, C. Correale, M. Allocca, G. Fiorino, M. Argollo, A. Zilli, E. Zacharopoulou, L. Loy, G. Roda, S. Danese, TL1A: A new potential target in the treatment of inflammatory bowel disease. Curr. Drug Targets. 22, 760–769 (2021).
62. V. Solitano, V. Jairath, F. Ungaro, L. Peyrin-Biroulet, S. Danese, TL1A inhibition for inflammatory bowel disease treatment: From inflammation to fibrosis. MED. 5, 386–400 (2024).
63. S. Jin, J. Chin, S. Seeber, J. Niewoehner, B. Weiser, N. Beaucamp, J. Woods, C. Murphy, A. Fanning, F. Shanahan, K. Nally, R. Kajekar, A. Salas, N. Planell, J. Lozano, J. Panes, H. Parmar, J. DeMartino, S. Narula, D. A. Thomas-Karyat, TL1A/TNFSF15 directly induces proinflammatory cytokines, including TNFα, from CD3+CD161+ T cells to exacerbate gut inflammation. Mucosal Immunol. 6, 886–899 (2013).
64. V. Valatas, G. Kolios, G. Bamias, TL1A (TNFSF15) and DR3 (TNFRSF25): A Co-stimulatory System of Cytokines With Diverse Functions in Gut Mucosal Immunity. Front. Immunol. 10, 583 (2019).
65. M. Hassan-Zahraee, Z. Ye, L. Xi, M. L. Baniecki, X. Li, C. L. Hyde, J. Zhang, N. Raha, F. Karlsson, J. Quan, D. Ziemek, S. Neelakantan, C. Lepsy, J. R. Allegretti, J. Romatowski, E. J. Scherl, M. Klopocka, S. Danese, D. E. Chandra, U. Schoenbeck, K. E. Hung, Antitumor Necrosis Factor-like Ligand 1A Therapy Targets Tissue Inflammation and Fibrosis Pathways and Reduces Gut Pathobionts in Ulcerative Colitis. Inflamm. Bowel Dis. 28, 434–446 (2022).
66. S. Kany, J. T. Vollrath, B. Relja, Cytokines in inflammatory disease. Int. J. Mol. Sci. 20 (2019), doi:10.3390/ijms20236008.
67. I. F. Charo, R. M. Ransohoff, The many roles of chemokines and chemokine receptors in inflammation. N. Engl. J. Med. 354, 610–621 (2006).
68. P. A. Morel, R. E. C. Lee, J. R. Faeder, Demystifying the cytokine network: Mathematical models point the way. Cytokine. 98, 115–123 (2017).
69. I. B. McInnes, E. M. Gravallese, Immune-mediated inflammatory disease therapeutics: past, present and future. Nat. Rev. Immunol. 21, 680–686 (2021).
70. K. Kveler, E. Starosvetsky, A. Ziv-Kenet, Y. Kalugny, Y. Gorelik, G. Shalev-Malul, N. Aizenbud-Reshef, T. Dubovik, M. Briller, J. Campbell, J. C. Rieckmann, N. Asbeh, D. Rimar, F.

Meissner, J. Wiser, S. S. Shen-Orr, Immune-centric network of cytokines and cells in disease context identified by computational mining of PubMed. Nat. Biotechnol. 36, 651–659 (2018).
71. M. B. Atallah, V. Tandon, K. J. Hiam, H. Boyce, M. Hori, W. Atallah, M. H. Spitzer, E. Engleman, P. Mallick, ImmunoGlobe: enabling systems immunology with a manually curated intercellular immune interaction network. BMC Bioinformatics. 21, 346 (2020).
72. K. Sommer, M. Wiendl, T. M. Müller, K. Heidbreder, C. Voskens, M. F. Neurath, S. Zundler, Intestinal Mucosal Wound Healing and Barrier Integrity in IBD-Crosstalk and Trafficking of Cellular Players. Front Med (Lausanne). 8, 643973 (2021).
73. E. Bartee, G. McFadden, Cytokine synergy: an underappreciated contributor to innate anti-viral immunity. Cytokine. 63, 237–240 (2013).
74. E. Armingol, A. Officer, O. Harismendy, N. E. Lewis, Deciphering cell–cell interactions and communication from gene expression. Nat. Rev. Genet. (2020), doi:10.1038/s41576-020-00292-x.
75. P. S. L. Schäfer, D. Dimitrov, E. J. Villablanca, J. Saez-Rodriguez, Integrating single-cell multi-omics and prior biological knowledge for a functional characterization of the immune system. Nat. Immunol. 25, 405–417 (2024).
76. H. Daneshpour, H. Youk, Modeling cell-cell communication for immune systems across space and time. Current Opinion in Systems Biology. 18, 44–52 (2019).
77. C. G. Williams, H. J. Lee, T. Asatsuma, R. Vento-Tormo, A. Haque, An introduction to spatial transcriptomics for biomedical research. Genome Med. 14, 68 (2022).
78. I. Kleino, P. Frolovaitė, T. Suomi, L. L. Elo, Computational solutions for spatial transcriptomics. Comput. Struct. Biotechnol. J. 20, 4870–4884 (2022).
79. E. Armingol, A. Ghaddar, C. J. Joshi, H. Baghdassarian, I. Shamie, J. Chan, H.-L. Her, S. Berhanu, A. Dar, F. Rodriguez-Armstrong, O. Yang, E. J. O'Rourke, N. E. Lewis, Inferring a spatial code of cell-cell interactions across a whole animal body. PLoS Comput. Biol. 18, e1010715 (2022).
80. G. Palla, D. S. Fischer, A. Regev, F. J. Theis, Spatial components of molecular tissue biology. Nat. Biotechnol. 40, 308–318 (2022).
81. I. Hautefort, M. Poletti, D. Papp, T. Korcsmaros, Everything You Always Wanted to Know About Organoid-Based Models (and Never Dared to Ask). Cell. Mol. Gastroenterol. Hepatol. 14, 311–331 (2022).
82. D. Papp, T. Korcsmaros, I. Hautefort, Revolutionising immune research with organoid-based co-culture and chip systems. Clin. Exp. Immunol. (2024), doi:10.1093/cei/uxae004.
83. T. Recaldin, L. Steinacher, B. Gjeta, M. F. Harter, L. Adam, K. Kromer, M. P. Mendes, M. Bellavista, M. Nikolaev, G. Lazzaroni, R. Krese, U. Kilik, D. Popovic, B. Stoll, R. Gerard, M. Bscheider, M. Bickle, L. Cabon, J. G. Camp, N. Gjorevski, Human organoids with an autologous tissue-resident immune compartment. Nature. 633, 165–173 (2024).
84. J.-P. Villemin, L. Bassaganyas, D. Pourquier, F. Boissière, S. Cabello-Aguilar, E. Crapez, R. Tanos, E. Cornillot, A. Turtoi, J. Colinge, Inferring ligand-receptor cellular networks from bulk and spatial transcriptomic datasets with BulkSignalR. Nucleic Acids Res. 51, 4726–4744 (2023).
85. Y. Hao, T. Stuart, M. H. Kowalski, S. Choudhary, P. Hoffman, A. Hartman, A. Srivastava, G. Molla, S. Madad, C. Fernandez-Granda, R. Satija, Dictionary learning for integrative, multimodal and scalable single-cell analysis. Nat. Biotechnol. 42, 293–304 (2024).
86. S. Mangiola, M. A. Doyle, A. T. Papenfuss, Interfacing Seurat with the R tidy universe. Bioinformatics. 37, 4100–4107 (2021).

87. J. Kinchen, H. H. Chen, K. Parikh, A. Antanaviciute, M. Jagielowicz, D. Fawkner-Corbett, N. Ashley, L. Cubitt, E. Mellado-Gomez, M. Attar, E. Sharma, Q. Wills, R. Bowden, F. C. Richter, D. Ahern, K. D. Puri, J. Henault, F. Gervais, H. Koohy, A. Simmons, Structural remodeling of the human colonic mesenchyme in inflammatory bowel disease. Cell. 175, 372-386.e17 (2018).
88. K. Parikh, A. Antanaviciute, D. Fawkner-Corbett, M. Jagielowicz, A. Aulicino, C. Lagerholm, S. Davis, J. Kinchen, H. H. Chen, N. K. Alham, N. Ashley, E. Johnson, P. Hublitz, L. Bao, J. Lukomska, R. S. Andev, E. Björklund, B. M. Kessler, R. Fischer, R. Goldin, A. Simmons, Colonic epithelial cell diversity in health and inflammatory bowel disease. Nature. 567, 49–55 (2019).
89. D. Corridoni, A. Antanaviciute, T. Gupta, D. Fawkner-Corbett, A. Aulicino, M. Jagielowicz, K. Parikh, E. Repapi, S. Taylor, D. Ishikawa, R. Hatano, T. Yamada, W. Xin, H. Slawinski, R. Bowden, G. Napolitani, O. Brain, C. Morimoto, H. Koohy, A. Simmons, Single-cell atlas of colonic CD8+ T cells in ulcerative colitis. Nat. Med. 26, 1480–1490 (2020).
90. P. Shannon, A. Markiel, O. Ozier, N. S. Baliga, J. T. Wang, D. Ramage, N. Amin, B. Schwikowski, T. Ideker, Cytoscape: a software environment for integrated models of biomolecular interaction networks. Genome Res. 13, 2498–2504 (2003).
91. E. Paradis, J. Claude, K. Strimmer, APE: Analyses of Phylogenetics and Evolution in R language. Bioinformatics. 20, 289–290 (2004).
92. I. Letunic, P. Bork, Interactive Tree Of Life (iTOL) v5: an online tool for phylogenetic tree display and annotation. Nucleic Acids Res. 49, W293–W296 (2021).
93. D. P. Gil, J. N. Law, T. M. Murali, The PathLinker app: Connect the dots in protein interaction networks. [version 1; peer review: 1 approved, 2 approved with reservations]. F1000Res. 6, 58 (2017).
94. Andrews S., Babraham Bioinformatics - FastQC A Quality Control tool for High Throughput Sequence Data. Babraham Bioinformatics (2010), (available at https://www.bioinformatics.babraham.ac.uk/projects/fastqc/).
95. A. Dobin, C. A. Davis, F. Schlesinger, J. Drenkow, C. Zaleski, S. Jha, P. Batut, M. Chaisson, T. R. Gingeras, STAR: ultrafast universal RNA-seq aligner. Bioinformatics. 29, 15–21 (2013).
96. Y. Liao, G. K. Smyth, W. Shi, featureCounts: an efficient general purpose program for assigning sequence reads to genomic features. Bioinformatics. 30, 923–930 (2014).
97. P. Ewels, M. Magnusson, S. Lundin, M. Käller, MultiQC: summarize analysis results for multiple tools and samples in a single report. Bioinformatics. 32, 3047–3048 (2016).
98. M. I. Love, W. Huber, S. Anders, Moderated estimation of fold change and dispersion for RNA-seq data with DESeq2. Genome Biol. 15, 550 (2014).
99. T. Sato, D. E. Stange, M. Ferrante, R. G. J. Vries, J. H. Van Es, S. Van den Brink, W. J. Van Houdt, A. Pronk, J. Van Gorp, P. D. Siersema, H. Clevers, Long-term expansion of epithelial organoids from human colon, adenoma, adenocarcinoma, and Barrett's epithelium. Gastroenterology. 141, 1762–1772 (2011).
100. G. M. Jowett, E. Read, L. B. Roberts, D. Coman, M. Vilà González, T. Zabinski, U. Niazi, R. Reis, T.-J. Trieu, D. Danovi, E. Gentleman, L. Vallier, M. A. Curtis, G. M. Lord, J. F. Neves, Organoids capture tissue-specific innate lymphoid cell development in mice and humans. Cell Rep. 40, 111281 (2022).
101. E. H. Kromann, G. M. Jowett, J. F. Neves, Expansion and Maturation of Innate Lymphoid Cell Precursors Using Human iPSC-Derived Intestinal Organoids. Methods Mol. Biol. (2024), doi:10.1007/7651_2024_568.

102. A. Leha, N. Moens, R. Meleckyte, O. J. Culley, M. K. Gervasio, M. Kerz, A. Reimer, S. A. Cain, I. Streeter, A. Folarin, O. Stegle, C. M. Kielty, HipSci Consortium, R. Durbin, F. M. Watt, D. Danovi, A high-content platform to characterise human induced pluripotent stem cell lines. Methods. 96, 85–96 (2016).
103. K. W. McCracken, J. C. Howell, J. M. Wells, J. R. Spence, Generating human intestinal tissue from pluripotent stem cells in vitro. Nat. Protoc. 6, 1920–1928 (2011).
104. J. R. Spence, C. N. Mayhew, S. A. Rankin, M. F. Kuhar, J. E. Vallance, K. Tolle, E. E. Hoskins, V. V. Kalinichenko, S. I. Wells, A. M. Zorn, N. F. Shroyer, J. M. Wells, Directed differentiation of human pluripotent stem cells into intestinal tissue in vitro. Nature. 470, 105–109 (2011).
105. Y.-H. Tsai, R. Nattiv, P. H. Dedhia, M. S. Nagy, A. M. Chin, M. Thomson, O. D. Klein, J. R. Spence, In vitro patterning of pluripotent stem cell-derived intestine recapitulates in vivo human development. Development. 144, 1045–1055 (2017).
106. K. B. Jung, H. Lee, Y. S. Son, M.-O. Lee, Y.-D. Kim, S. J. Oh, O. Kwon, S. Cho, H.-S. Cho, D.-S. Kim, J.-H. Oh, M. Zilbauer, J.-K. Min, C.-R. Jung, J. Kim, M.-Y. Son, Interleukin-2 induces the in vitro maturation of human pluripotent stem cell-derived intestinal organoids. Nat. Commun. 9, 3039 (2018).
107. G. Korotkevich, V. Sukhov, N. Budin, B. Shpak, M. N. Artyomov, A. Sergushichev, Fast gene set enrichment analysis. BioRxiv (2016), doi:10.1101/060012.
108. A. Kassambara, ggpubr: "ggplot2" Based Publication Ready Plots (2023), (available at https://rpkgs.datanovia.com/ggpubr/).
109. D. Pratt, J. Chen, R. Pillich, V. Rynkov, A. Gary, B. Demchak, T. Ideker, Ndex 2.0: A clearinghouse for research on cancer pathways. Cancer Res. 77, e58–e61 (2017).
110. L. Broutier, A. Andersson-Rolf, C. J. Hindley, S. F. Boj, H. Clevers, B.-K. Koo, M. Huch, Culture and establishment of self-renewing human and mouse adult liver and pancreas 3D organoids and their genetic manipulation. Nat. Protoc. 11, 1724–1743 (2016).
111. C. M. Cattaneo, K. K. Dijkstra, L. F. Fanchi, S. Kelderman, S. Kaing, N. van Rooij, S. van den Brink, T. N. Schumacher, E. E. Voest, Tumor organoid-T-cell coculture systems. Nat. Protoc. 15, 15–39 (2020).

Acknowledgments: We thank the past and present members of the Korcsmaros and Powell groups, the participants of the Interdisciplinary Signaling Workshop 2023, and D. Cozzetto for their advice and suggestions regarding our work. We thank the NIHR Imperial BRC Organoid Facility for their support of the organoid work, and the Earlham Institute Technical Genomics group for their work involving RNA-sequencing. The RSpo1-Fc cell line was a gift from C. Kuo (Stanford University, USA) and the Noggin cell line was a gift from the Hubrecht Institute. We would like to thank T. Poobalasingam from Biolegend for their assistance with processing the LegendPlex assay data. The authors wish to acknowledge the support of the LMS/NIHR Flow Facility at Imperial College London. **Funding:** T.K. and I.H. were supported by the NIHR Imperial Biomedical Research Centre Organoid Facility and the UKRI BBSRC Gut Microbes and Health Institute Strategic Program BB/R012490/1 and its constituent projects, BBS/E/F/000PR10353 and BBS/E/F/ 000PR10355, as well as a UKRI BBSRC Core Strategic Program Grant for Genomes to Food Security (BB/CSP1720/1) and its constituent work packages, BBS/E/T/000PR9819 and BBS/E/T/ 000PR9817. B.B, T.K., and I.H. were also supported by the UKRI BBSRC Institute Strategic Programme Food Microbiome and Health BB/X011054/1 and its constituent project, BBS/E/F/000PR13631. D.M. acknowledges financial support from Imperial College London

through an Imperial College Research Fellowship grant award. A.S. received funding from the International Organisation of Inflammatory Bowel Disease and St Mark's Hospital Foundation. J.P.T, is supported by the Chain-Florey Clinical PhD Fellowship jointly funded by the National Institute for Health Research (NIHR) Imperial Biomedical Research Centre (BRC) and the UKRI Medical Research Council (MRC) Laboratory of Medical Sciences (LMS). N.P. was supported by the Wellcome Trust (WT101159 and 225875). N.P., A.S., and H.I. were supported by the National Institute for Health Research (NIHR) Imperial Biomedical Research Centre (BRC). The views expressed are those of the authors and not necessarily those of the NIHR or the UK Department of Health and Social Care. D.C. and J.F.N. acknowledge funding from The Leona M. and Harry B. Helmsley Charitable Trust. J.F.N. also acknowledges funding from the Lister Institute of Preventive Medicine and the BBSRC/NCR3 (NC/X002497/1). E.H.K. acknowledges a PhD studentship from the Mechanics of Life Leverhulme Doctoral Scholarship Programme at King's College London. D.C., E.H.K., and J.F.N. also acknowledge support by Research and Development, Guy's and St Thomas' NHS Foundation Trust through the advanced cytometry platform. The views expressed are those of the author(s) and not necessarily those of the NHS. **Author contributions:** Conceptualization: M.O. and T.K. Software: M.O., L.C., and B.B. Validation: I.H., A.S., H.I., D.C., E.H.K., D.P., and S.S.K. Analysis: M.O., J.P.T., D.M., D.C., E.H.K., and S.S.K. Writing: M.O., J.P.T., I.H., D.C., E.H.K., D.M., and T.K. Supervision: T.K., N.P., J.F.N., and D.P. Funding acquisition: T.K., N.P., and J.F.N. **Competing interests:** A.S. has received travel expense funding from Janssen and Alfasigma, and speaker expenses from Alfasigma and Ferring Pharmaceuticals. N.P. has received research grant(s) from Bristol Myers Squibb and reports personal fees from Takeda, Janssen, Pfizer, Bristol-Myers Squibb, Abbvie, Roche, Lilly, Allergan, and Celgene, outside the submitted work. N.P. has served as a speaker/advisory board member for Abbvie, Allergan, Bristol Myers Squibb, Celgene, Falk, Ferring, Janssen, Pfizer, Tillotts, Takeda and Vifor Pharma. J.F.N. is inventor on a patent application related to this work (no. WO 2024/256627). The other authors declare that they have no competing interests. **Data and materials availability:** The code used to generate the cytokine–cytokine interactions, figures, data, and the subsequent analysis can be accessed in the project github repository (https://github.com/korcsmarosgroup/ulcerative-colitis-cytokine-networks) and zenodo (10.5281/zenodo.15297794). The generated cytokine networks can also be interactively accessed on the NDEx platform (109). RNAseq data have been deposited to ENA: PRJEB94055. 293T-HA-RSpo1-Fc cells are available from Leland Stanford Junior University under a material transfer agreement with the University. HEK293-mNoggin-Fc cells are available from Hubretch Institute/KNAW under a material transfer agreement with the Institution.

Fig. 1. Generating condition-specific cytokine networks in UC. (**A**) The computational pipeline processes data from the scRNA-seq IBD atlas scIBD. Data were processed with NicheNet, with the gene set of interest set to a list of cytokines. It connected active cytokine ligands to their putative cytokine targets, resulting in condition-specific cytokine networks. (**B**) Hierarchical clustering of networks according to disease and treatment status. The generated networks were

comparable in size, with the inflamed, treatment-naive network having the largest number of interactions. (**C**) Network visualization displaying all generated interactions in the networks, and highlighting the cytokines with the largest number of interactions (highest degree). The employed centrality network layout emphasizes betweenness centrality, a measure of how often each cytokine appears on the shortest paths connecting other cytokines in the network. The most central cytokines are positioned closer to the center.

Fig. 2. Validation of cytokine-cytokine interactions. (**A**) Comparison of target sets of xxx between predicted interactions and differential expression results from the Immune Dictionary resource of Cui *et al*. (23). Twelve of the twenty shared source cytokines had significantly overlapping target sets. (**B**) Enrichment plot showing the enrichment of IFN-γ targets among differentially expressed genes from patient-derived inflamed colonic organoids treated with IFN-γ. Data are from organoids from four donors. (**C**) Enrichment of target sets of multiple cytokine genes in inflamed, noninflamed, and healthy colonic organoid transcriptomics data. Normalized Enricment Score (NES) quantifies the degree of enrichment. (**D**) Downstream cytokines with significantly altered protein amounts after co-culture of xxx with ILC1s . (n=3 for standalone, n = 4 for ILC1 co-cultures). We observed a significant change in protein concentration for 57% of predicted targets (Wilcoxon Rank Sum test, p-value <= 0.05). Supplementary Figure 3 details p-values for all measured cytokines.

Fig. 3. A specific subnetwork of cytokine-cytokine interactions characterizes treatment-naive inflamed UC tissues. (**A**) Jaccard index distribution of cytokine-cytokine interactions. For each cytokine-cytokine interaction the Jaccard-index measures the overlap in contributing cell types (as

source or target) between the disease condition and healthy controls. The inflamed treatment-naive condition shows significantly lower median Jaccard indices that the inflamed treatment-exposed condition (median inflamed-naive = 0.27, n inflamed-naive = 493, median inflamed-treated = 0.38, n inflamed-treated = 422, Wilcoxon-Rank Sum test $P < 1.6e-06$). (**B**) Degree and betweenness centrality differences between inflamed treatment-naive and treatment-exposed networks. (**C**) Cytokine interaction subnetwork containing interactions exclusively present in inflamed treatment-naive ulcerative colitis patients. Nodes are arranged hierarchically, to show the direction of information flow through the cytokine network. (**D**) Bar plots showing the in-degree (incoming interactions, top) and out-degree (outgoing interactions, bottom) of nodes in the cytokine subnetwork exclusive to inflamed treatment-naive ulcerative colitis patients. (**E**) Cytokines with currently targeted by biologic agents (TNF, IL23A) in the treatment-naive state.

Fig. 4. Cytokine network rewiring and shared interactions. (**A**) Distribution of degree-corrected rewiring scores ascertained through the DyNet network rewiring algorithm. The top-scoring cytokines are highlighted. (**B**) The top rewired nodes shared across all networks (**C**) Representation of the first neighbors of the rewired nodes IL-22 and OSM in tissues of the indicated sources. Interactions are coloured according to the compared states. Dashed lines refer to interactions found exclusively in UC, solid lines are present in all networks. (**D**) Missing (left) and shared (right) subnetworks in UC. The largest connected components of the missing (exclusive to healthy) and shared (exclusive to UC) interactions are shown next to the Venn-diagrams. The number of shared interactions, and their percentage share is shown in the Venn-diagrams.

Fig. 5. JAK paralog specificity of cytokine networks. (**A**) Left: The numbers of JAK proteins used by the generated cytokine-cytokine interactions. Right: The ratio of usage of the indicated JAK proteins per cytokine-cytokine interaction type. (**B**) List of the known JAK protein usage preferences of the indicated cytokines, and the percentage of correctly identified JAKs in the predicted intracellular signaling pathways. (**C**) DyNet rewiring compared to the inflamed-naive network after the removal of cytokine interactions mediated by the indicated JAK paralogs. Only the top values are shown. (**D**) Analysis of the effect of removing the indicated JAK protein interactions (through the use of specific inhibitors) on cytokine networks involving IL-22 and OSM in the UC inflamed, treatment-naive condition.

Fig. 6. TL1A as a drug target in the treatment-naive cytokine network. (**A**) The UC inflamed treatment-naive cytokine network with the OpenTargets global score overlaid on the cytokines. (**B**) List of the highest OpenTargets global score of cytokines and the availability of UC drugs. (**C**) Scatterplot of the $\log_2$ edge weight values compared to the healthy controls and the Jaccard index of cell type similarity compared to the healthy condition. (**D**) Cell types contributing to the expanded TL1A-TNF interaction among healthy controls and UC inflamed, treatment-naive conditions. (**E**) First neighbors of TL1A in the inflamed treatment-naive network. UC-specific interactions are shown with dashed lines. (**F**) Interactions from TL1A to all significantly affected cytokines after anti-TL1A treatment as shown by Hassan-Zahraee *et al*. (65).